European Polymer Journal 129 (2020) 109621

Contents lists available at ScienceDirect

European Polymer Journal

journal homepage: www.elsevier.com/locate/europolj

Polymer scaffolds as drug delivery systems

Italo Rodrigo Calori[a,d], Gustavo Braga[a], Priscila da Costa Carvalho de Jesus[b], Hong Bi[c], Antonio Claudio Tedesco[c,d,*]

[a] Department of Chemistry, Research Nucleus in Photodynamic Systems, State University of Maringá, Av. Colombo 5790, Maringá, Paraná 97020-900, Brazil
[b] University of São Paulo, Polytechnic School. Av. Prof. Lineu Prestes, 580, Building Semi-Industrial University City, 05434070 São Paulo, SP, Brazil
[c] School of Chemistry and Chemical Engineering, Anhui Key Laboratory of Modern Biomanufacturing, Anhui University, Hefei 230601, China
[d] Department of Chemistry, Center of Nanotechnology and Tissue Engineering -Photobiology and Photomedicine Research Group, Faculty of Philosophy, Sciences and Letters of Ribeirão Preto, University of São Paulo, Ribeirão Preto, São Paulo 14040-901, Brazil

ARTICLE INFO

Keywords:
Polymeric implants
Injectables
Biomaterials
Bone regeneration
Electrospinning

ABSTRACT

Drug delivery scaffolds are smart alternatives to conventional formulations and allow for controlled spatio-temporal releases of active compounds. In several fields of human health, various methods have emerged with natural and synthetic polymers that make the fabrication of new polymer scaffolds possible. This review provides an overview of all recently published studies on the development and application of polymer scaffolds targeting controlled drug delivery in medicinal fields, including regenerative medicine and cancer therapy. The review includes a summary of the most common types of polymers used in drug release scaffolds, polymer scaffold classes, and the most common fabrication methods employed to develop such scaffolds. A detailed overview is provided concerning the strategies used to load drugs into scaffolds and their effects on drug release. A discussion about the strategies applied to modulate drug delivery is introduced. This details polymer blends and responsive releases that target the control of the drug delivery rate. In addition, current examples of their applications are provided. These include anti-inflammatory drugs and growth factors, as well as more recent *in vitro* and *in vivo* assays. Finally, future perspectives of these biomedical devices in clinical applications are presented.

1. Introduction

The advances of polymer materials over the last century have led to the possibility of their biomedical applications. These systems are presented as platforms for advanced medical devices, drug delivery systems (DDS), and as key tools for the novel technologies in regenerative medicine and tissue engineering. The wide spectrum of materials for several fields of human health comes from the current available variety of natural and synthetic polymers [1]. This has also been promoted with the emergence of novel strategies from the most traditional casting-based methods to the recent three-dimensional (3DP) techniques that have facilitated the fabrication of materials with different interpenetrating networks, porosities, pore sizes, and channels. Along with the those mentioned above, the biocompatibilities, structural similarities with the target tissue, and mechanical properties form the driving forces of the application of polymer materials in medicine [2].

The rational approach of the material researchers has led to the design of implant or injectable polymer platforms, which are now called polymer scaffolds. Polymer implants are pre-fabricated forms (flexible or not) of two or three dimensions comprised of single or blend polymers with the function of repairing tissues or curing illnesses. In parallel, a polymer injectable colloidal solution can form hydrogels of a 3D network *in situ* by hydrophobic interactions or a crosslink of groups of the polymer chains. The use of an injectable allows for the opportunity of minimal incision sizes and closings with anatomical efficacy [3], which can be difficult to obtain with thick solid forms of pre-fabrication even with 3DP technologies. The unique properties of polymers assist the design of stretchable and deformable films and membranes that permit a dynamic shape adaptation of the device. This makes them advantageous compared to other scaffold-production materials, including with glass and ceramic [4,5]. Even in composites, a polymer matrix is essential to meet appropriate mechanical properties [6], bioresorbabilities, and specific drug release profiles. This can prevent a post-treatment step of removal surgery and makes them appropriate as spatiotemporal DDS [7,8].

A DDS can be described as any platform that loads active compounds and releases them in the target tissue to enhance safety and

* Corresponding author.
E-mail address: atedesco@usp.br (A.C. Tedesco).

https://doi.org/10.1016/j.eurpolymj.2020.109621
Received 10 September 2019; Received in revised form 12 March 2020; Accepted 13 March 2020
Available online 19 March 2020
0014-3057/

efficacy of the drug [9]. The primary intent of a DDS is to maintain the drugs at optimal therapeutic levels in the body during the treatment. This can prevent multiple administrations. In this scenario, polymer implants are ideal for drug delivery.. They release one or more active compounds in a desired release rate throughout the time of the therapy. Also, scaffolds provide drug protection in the body before release. This is also important to prevent side effects during the controlled release and fluctuations of drug levels from multiple sequential administrations of immediate drug releases. This is even more relevant as the drug content increases. Because scaffolds are implanted on a site-specific basis, a more controlled spatiotemporal release of active compounds can be obtained when compared to conventional formulations [10,11]. In addition to drugs, biocompatible scaffolds are currently used to release cells, proteins, and genes [12,13]. These applications expand their limits for the designing of novel treatments for diseases. These include treatments for tumors and pathogen-derived microbials, and the stimulation of biological responses in regenerative medicine as a device of tissue repair.

Polymer scaffolds can provide cell attachment and proliferation. The physical bonds between biological parts and scaffolds lead to healing and integration of the tissue [14]. Targeting accelerates these processes. Polymer-based scaffolds have been used as reservoirs to load and deliver key proteins of the transforming growth factor beta (TGF-β) superfamily. These include osteogenic and differentiation factors, as well as angiogenic factors [15–17]. Good results led to the first US Food and Drug Administration (FDA) approval for collagen implant loading growth factors, including bone morphogenetic protein 2 (BMP-2) (Medtronic's INFUSE®) in 2002.

Faced with such a wide spectrum of applications, this review aims to provide an overview of recent published studies on the development and potential of polymer scaffolds applied to controlled, sustained, and on-demand DDS. The following discussion is not intended to exhaust the current knowledge on this topic, but rather supply an overall insight to inspire biomaterial scientists to consider the advances in polymer-based drug delivery scaffolds.

2. Common polymers

Polymers are macromolecules characterized by the chemical junction of repeated short units that are named monomers when isolated. The current literature shows a variety of classifications for the polymers. One of the most common modes classifies polymers into two large groups, according to their origin as natural or synthetic polymers. Examples of natural polymers are proteins (including collagen, gelatin, elastin, keratin, and silk fibroin) and polysaccharides (such as hyaluronic acid, alginate, and chitosan). Synthetic polymers include polylactic acid, polyvinilalchool, and polycaprolactone (PCL).

2.1. Natural polymers

Natural polymers are polymeric units typically extracted from living organisms [18]. Most natural polymers are used in scaffolds that target hydrophilic characteristics. Such characteristics include sufficient biocompatibility, a biofriendly solvent-based method, and non-toxic degradation. They are mostly used in the production of hydrogels and as blends in pre-formed solid scaffolds.

2.1.1. Proteins

2.1.1.1. Silk fibroin (SF). SF is a natural biofiber extracted mainly from insects, spiders [19], and silkworms (such as Bombyx mori) [20]. Its structure presents H-chain, L-chain, and glycoprotein P25 [21]. SF side chains have several reactive amino acids, such as serine, threonine, aspartic, glutamic, and tyrosine. These are useful sites for chemical and functional modification strategies. The amino acid sequences are arranged in repetitive glycine-alanine-glycine-alanine-glycine-serine (Gly-Ala-Gly-Ala-Gly-Ser) moieties, and their self-assembly provides a highly crystalline anti-parallel β-sheet structure [22].

The hydrogen bonds and van der Waals interactions between stacked β-sheets give the material promising mechanical properties for biomedical applications. The extent of the β-sheet structure can be controlled through physical or chemical methods that are responsible for the crystallinity and degradation rates. Mainly at the physiological pH and basic media, a deprotonation of Tyr side groups occurs. This makes the SF amorphous due to decreased hydrogen bonds [23] and facilitates the biodegradability processes. In acidic conditions, because the hydrogen bonds [23], the crystalline domains of the β-sheet structure are promoted and prevent the penetration of water and proteases. This results in slow biodegradation of silk *in vivo* [24].

SF has been applied in biomaterial research, including with films, hydrogels, nanoparticles, and other DDS. SF has drawn attention for its use in the fabrication of scaffolds for application in neuroengineering [25,26]. This is due to its potential to mimic *in vivo* microenvironments and to provide adjustable biomaterials for soft nervous tissue reconstruction. This allows for the complete filling of amorphous cavities from brain or surgery injuries and leads to consistent therapeutic effects in brain tissue. Also, SF has allowed for tunable 3D bioengineered SF brain tissue platforms. These serve as versatile tumor tissue systems for the evaluation of the stages and mechanisms of the microenvironmental roles in pediatric ependynoma brain tumors and glioblastoma progression [27].

Other recent applications of SF scaffolds include scaffolds for the release of growth factors, such as stromal-derived factor-1α (SDF-1α)/transforming growth factor-β1 (TGF-β1)-loaded silk fibroin-porous gelatin scaffolds for the promotion of favorable microenvironments for cartilage injury repair [28]. SF discs are being developed as biomaterials to encapsulate and release antibodies (IgG) and HIV inhibitor 5P12-RANTES. This is a useful tool to prevent HIV infection and minimize the pandemic [29]. Translucid SF hydrogels are used as matrixes to load and release the photosensitizer 5-(4-aminophenyl)-10,15,20-tris-(4-sulphonatophenyl) porphyrin trisodium. The system is responsible for the generation of oxygen reactive species against neoplastic tissue in a clinical modality known as photodynamic therapy. The encapsulation of such porphyrin in the matrix of hydrogel prevents the aggregation process and increases the generation of singlet oxygen, promoting the photodynamic perspectives [30]. Tunable 3D bioengineered SF brain tissue platforms are used as versatile tumor tissue systems to evaluate the stages and mechanisms of microenvironmental roles in pediatric ependymoma brain tumors and glioblastoma progression [27].

2.1.1.2. Collagen. Collagen, or tropocollagen, is another amino acid-based macromolecule. It is the most abundant protein on earth [31]. It is an heteropolymer-based macromolecule that compounds fibers of structural function in tissues of animals. It is abundant in extracellular matrixes, cartilages, tendons, bones, skin, and connective tissues [32]. Currently, there are 28 known types of collagen, and more than 80 percent of collagen is disposed by the human body. They are composed by types I, II, and III. They are fibril-forming and have a superior mechanical property [32]. Although collagen is quite insoluble in physiological media, an enhanced solubility can be obtained by lowering/increasing the pH. This is used to solubilize it in aqueous media.

Collagen molecules are structured by a triple polypeptide-based helix of repeating motif Gly-X-Y, with X and Y being amino acids. The majority of the amino acids are glycine, proline, and hydroxyproline, in which glycine plays a key role in the packaging of the polymer chain. Each tropocollagen is around 300 nm in length and 1.5 nm of diameter, [31] with approximately 1,050 amino acids. Several tropocollagen organize themselves in fibrils of around 1 μm that organize further to form collagen fibers of approximately 10 μm. It is accepted that the formation of collagen fibrils enhances the strength and deformation, creating tough and robust material [31].

The promising characteristics of collagen encouraged material

researchers to use it in scaffolds in a variety of applications, such as for bone regeneration and as matrixes for cell growth. Their use as scaffolds started in 1881 through the targeting of biodegradable sutures in regenerative medicine. Currently, collagen scaffolds are used for sponge materials, gels, films, membranes, wound dressings, and skin replacements, among others. Collagen scaffolds with different density interfaces are being developed to promote neovascularization and rapid cellular invasion in tissue engineering, as well as to provide local gene delivery to multiple cell types [33].

2.1.2. Polysaccharides

The role of polysaccharides in plant and unicellular organisms is similar to the structural function of collagen in animals. A variety of macromolecules named polysaccharides can be obtained by chemical bonds through glycosidic linkage of several monosaccharide units. These can be identical (homopolysaccharides) or distinct units (heteropolysaccharides). Polysaccharides are widely used while targeting biocompatible hydrogels for biological applications and drug release when HA, alginate and chitosan are employed. Except for chitosan, these are anionic at the physiological pH because of the presence of glucuronic acid units. These yield solubility in physiological media. Their network structure (hydrogel) is kept in water by the crosslink of the polymer units. In particular, glucuronic acid gives rise to other important polymers that form anionic polysaccharides of animal, plant, and bacterial origin. From plants, polymer-based d-glucuronic acid promotes the formation of well-known hemicelluloses and gum arabic, mostly used as hydrogels in pharmaceuticals. Bacterial polysaccharides include xanthan (from *Xanthomonas sp*.) and *ardisicrenoside E* (produced by *Ardisia crenata*). Heparan sulfate, chondroitin 4- and 6-sulfates, and HA are examples of polysaccharides with animal origins. However, microbial production processes have also been studied.

2.1.2.1. Hyaluronic acid. HA is one of the most important polysaccharide-based d-glucuronic acids. As the main component of the extracellular matrix is in the form of sodium hyaluronate, HA is a polysaccharide comprised of alternating units of glucuronic acid and N-acetylglucosamine. It is typically linked by β-1,3- and β-1,4-glycosidic bonds [34]. HA is commonly called hyaluronan in physiological media. This is a general term for the several forms that the molecule can assume. Due to its hydrodynamic properties, HA hydrogels have been widely used for cartilage tissue engineering [35] and wound healing [36]. As a delivery system of anti-cancer compounds, HA-based injectable hydrogels have been used for the local release of cisplatin [37], doxorubicin [38], paclitaxel [38,39], docetaxel [40], camptothecin [40], rapamycin [40], IFN-a2a [41], irinotecan [42], and 5-fluorouracil [42].

2.1.2.2. Alginate. Alginate is another polysaccharide that is based on glucuronic acid units. Alginates are found in seaweed. They are mostly extracted from brown algae (Phaeophyceae). They are present in the exopolysaccharide of *Pseudomonas aeruginosa* bacteria [43]. The natural copolymer (comprised of glucuronic and mannuronic acid) blocks the display characteristics. Such characteristics include polyelectrolytic, biocompatible, non-toxic, non-immunogenic, and antimicrobial states. Due to their capabilities as biomaterials for 3D cell culture systems, mainly in bone-tissue engineering, alginate scaffolds have been studied in combination with other polymers. These include collagen as a hybrid hydrogel for applications that can even target neurogenesis and neuronal maturation [43,44].

2.1.2.3. Chitosan. Chitosan is one of the most abundant natural amino polysaccharides. It is derived from a deacetylated form of native chitin obtained from crab and shrimp shells. Chitosan presents nontoxic, biocompatible, and biodegradable characteristics. It is also highly sensitive to water. It serves as a considerably versatile and promising biomaterial for application in biomedical fields, such as in wound healing, drug delivery, gene delivery, and tissue engineering. Due to its pKa value of around 6.5, chitosan is insoluble in physiological conditions. However, it presents enhanced solubility in acid media [45]. To yield water-soluble chitosan, structural modifications (including acetylation) can be used [46]. Chitosan presents insufficient mechanical strength. However, this disadvantage is overcome by blending chitosan and other natural polymers (such as collagen) to make it adequate for tissue engineering applications, such as in nerve regeneration. Chitosan also presents poor spinning performance. In electrospinning, chitosan is mostly used as a blend with polymers of higher spinning performance [47]. Recently, novel low molecular weight chitosan/PVA membranes have presented antibacterial properties[48].

The main disadvantage of some natural polymer-based scaffolds is their poor mechanical properties [49]. Due to this, a variety of natural polymers are modified or conjugated with active molecules to generate novel tailored polymers for biomedical applications [50]. Moreover, completely synthetic polymers are viable alternatives for tuning the properties of polymer scaffolds.

2.2. Synthetic polymers

A number of polymers have been fabricated by total synthesis, mostly by polymerization techniques [51]. The majority of synthetic polymers provide unique and important physical and chemical properties, and some of them are applied to the design of polymer-based drug delivery scaffolds. In particular, PCL, polylactic acid, and polyglycolic acid are widely used because of their controllable biodegradability, limited toxicity, and potential capability to generate porous scaffolds. However, limited cell adhesion occurs in some cases, including in the pure PCL matrix [52].

2.2.1. Polyesters

2.2.1.1. Polycaprolactone (PCL). PCL, an FDA-approved aliphatic and hydrophobic polyester, has considerable potential in biomedical applications due to its biocompatibility, printability as a thermo-ink for 3D printing, and its ability to form blends. PCL is also convenient for the drug delivery of many active compounds. Among its applications, PCL scaffolds have been studied as DDS for cancer, showing great potential against osteosarcoma. They are also applied to mimic the consistency of biological environments (such as ovarian tissue) to assist in surgical procedures.

2.2.1.2. Poly (lactic acid) (PLA). PLA is another hydrophobic aliphatic polyester. It was discovered in the seventeenth century by Carl Wilhelm Scheele, a Swedish chemist. PLA is a biocompatible and biodegradable polymer used in a broad range of applications. It has been approved by the FDA, and it is suitable for DDS, sutures, cell carriers, scaffolds, and many other biomedical devices. PLA scaffolds have been used as DDS for the release of prednisolone and dexamethasone for tissue regeneration [53], vascular endothelial growth (VEGF), with paclitaxel (PTX) for endothelialization acceleration, lumen stenosis prevention [54], with hydrochloride (PHMB) and Chlorhexidine (CHX) to inhibit bacterial growth [55], and with doxorubicin against tumors [56].

2.2.1.3. Poly (glycolic acid) (PGA). PGA is also an FDA-approved aliphatic polyester that is frequently used in the design of polymer materials. Since 1970, it has been available with the name Dexon®. It is more hydrophilic than PCL and PLA, being the first biodegradable material used in clinical applications as a suture. PGA fibrous scaffolds play a key role in the loading of monocyte chemoattractant protein-1 (MCP-1) for drug delivery during the treatment of wounds for diabetes patients [57]. Moreover, these scaffolds have potential in bone regeneration and tissue engineering. They are also commonly used as blends with other polymers, such as PLLA and PLA [58].

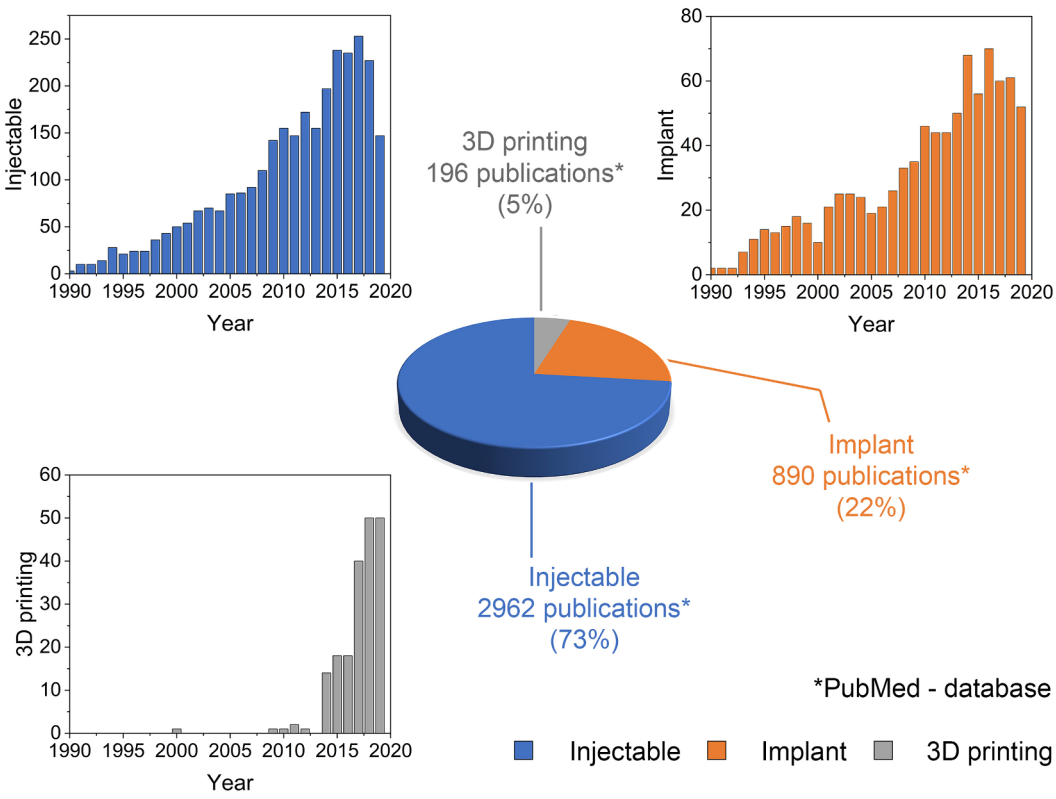

Fig. 1. Number of publications by year from 1990 to 2019 related to "drug delivery polymer," according to PubMed. The data were acquired by entering the following key words in the advanced search field of PubMed (data acquired on January 11, 2020): drug delivery polymer, injectable (blue), implant (orange), 3D printing (gray). (For interpretation of the references to colour in this figure legend, the reader is referred to the web version of this article.)

2.2.2. Polyalchools

2.2.2.1. Polyvinilalchool (PVA). PVA is a hydrophilic semicrystalline polymer that exhibits mechanical strength and biocompatibility. These properties make PVA a promising material for biological application, including for wound dressings, with membranes, surgical repairs, artificial skin, and correlated polymer scaffold materials. With respect to drug release, 3D hybrid PVA scaffolds obtained a sequential release of the antimicrobial agents rifampin, levofloxacin, and vancomycin, and presented good results against bacteria biofilms [59]. Other hybrid PVA/PEG scaffolds have shown great potential to release ciprofloxacin against the growth of microorganisms [60]. PVA scaffolds blended with PLA have been used to deliver a BMP-2 protein that targets bone regeneration [61].

2.2.3. Copolymers

Block copolymers are polymers that have two or more distinct polymer moieties linked to each other by covalent bonds. The possibility to assume different arrangements as ABA, BAB, or ABC for triblock copolymers and the distinct properties of different moieties make the copolymerization a key tool of tunable polymer properties. As an example, the hydrophobic behavior of PCL can be tunable by copolymerization and the creation of thermosensitive units where the degree of phase separation is dependent on the block lengths and co-block composition [62]. The addition of one or more poly(ethylene oxide) (PEO) segments in pre-formed hydrophobic polymers is also a frequent strategy used to enhance polymer hydrophilicity, modulate the mechanical properties, design nanoparticles, and develop novel thermoresponsive polymers for several purposes in biological applications [63,64]. Also, they are useful in 3DP technologies. These include the design of nerve guidance channels [65] and construction of bioprints for cartilage repair [66]. In drug release, polymer scaffolds with thermosensitive characteristics have a considerable impact against a series of illnesses and for regenerative medicines. They are discussed in the next topics.

First synthesized by Perret and Skoulios [67], recent studies have explored the FDA-approved PEG/PCL block copolymers as injectable thermosensitive hydrogels for local drug delivery [68]. While targeting novel properties, material researchers have synthesized a variety of other PCL copolymers of di-, tri-, or even with five blocks. These are comprised of two or more polymer moieties. They have been recently synthetized and include chitosan [69], poly(dimethylsiloxane) [62,70], poly(epichlorohydrin) [71], poly(l-lactide) [72], Poly(N-isopropylacrylamide)/poly(ethylene glycol) [73,74], poly(tetrahydrofuran) [75], poly(allyl ethylene phosphate) [76], n-butyl acrylate/methyl methacrylate [77], and oligosilsesquioxane [78]. Frequently, the copolymer terminals (mainly the OH− group) is used to covalently bond active compounds, including folic acid, biotin [79], and nitroxyl radicals [80].

2.2.3.1. Poly(lactic-co-Glycolic Acid) (PLGA). PLGA is a synthetic copolymer comprised of PLA and PGA moieties. It is characterized by a random chain. Thus, PLGA is a biodegradable polymer that combines with non-toxic metabolites, such as lactic acid and glycolic acid. Targeting biomedical applications, PLGA is used mainly as a polymer scaffold in tissue engineering. Also, it is applied as a material for DDS, orthopedic appliances, sutures, polymer scaffolds, and other biomedical circumstances. Recently, the PLGA scaffold exhibited regenerative capacity in renal tissues, providing potential for treatment of patients with renal dysfunction.

3. Classes of polymer scaffolds

The variety of polymers that can be used to design scaffolds allows for optimization according to the desired properties and applications.

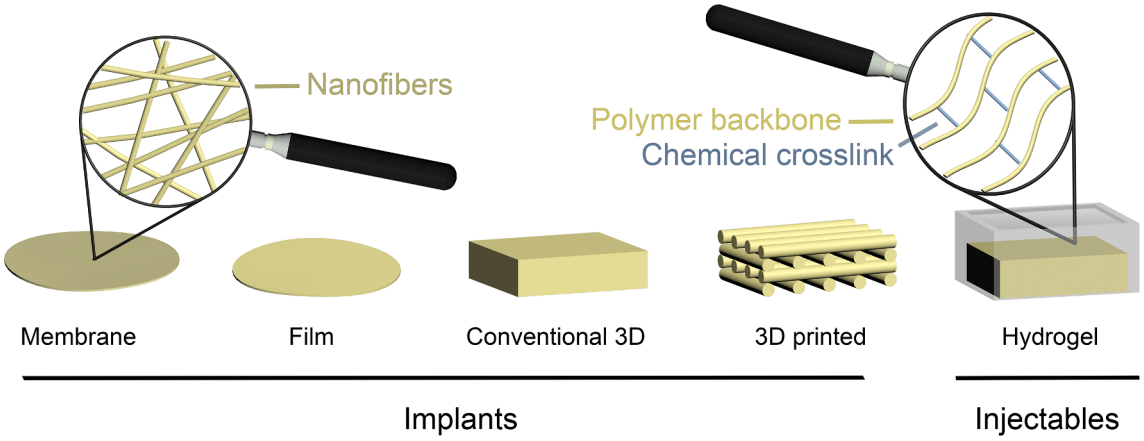

Fig. 2. Illustration of different classes of polymer scaffolds.

Moreover, functionalization regarding the tuning of their properties has expanded their spectra of applications. Thus, current polymer scaffolds have been comprised of a range of homopolymers, copolymers, modified polymers, and their blends. The number of studies that aim to design polymer scaffolds for drug delivery has grown since the nineties. Most of these studies target an injectable, as illustrated in Fig. 1.

Injectable scaffolds have been studied more than polymer implants as drug delivery polymer scaffolds in most cases due to their lower cost, ease of preparation, and ability to take the shape of a tissue defect. The latter prevents the necessity of patient-specific prefabrication. Moreover, as they are administered without surgical intervention, minimal discomfort is experienced by the patient [81]. Despite the large number of studies, polymer hydrogels have not been successful in clinical studies. This may be due to their low drug loading capacity, limited control of drug release, and non-ideal mechanical toughness. Moreover, the difficulty of degradation of highly crosslinked and efficient hydrogels [82] leads to partial drug release [83–85].

The classes of polymer implants involve polymer membranes, thin films, and conventional and printed 3D devices (mono- or multilayers) (Fig. 2). They differ in dimension (2 or 3D), thickness, and network. Also, film and 3D scaffolds can present a series of other characteristics, such as porosity and open channels. This is promising for drug release and integrated tissue–organ scaffolds for tissue engineering [86,87]. The differences come from the unique characteristics of each method of preparation. All of these properties affect drug release rates and can be used to achieve a desired drug release profile. Thus, a deep knowledge of each method and scaffold property is needed to optimize the drug release rate.

4. Common fabrication methods

A wide number of techniques is currently used to fabricate implantable and injectable scaffolds, ranging from the most traditional methods to the most modern 3D manufacturing approaches. The choice of a particular technique should be based on the nature of the polymer and drug, as well as the final characteristic and application desired. In this section, the authors present some of the most common techniques to design polymer scaffolds from implant to injectable.

4.1. Implantable scaffolds

Polymer-based implants can be fabricated by a large number of easy and economical techniques. A few of them are solvent casting, salt leaching, thermally-induced phase separation, electrospinning, polymer melt by a foaming process, freeze drying, rapid prototyping, and solid free-form fabrication. More recently, additive manufacturing for 3D printing has emerged as a promising tool to provide the most intricate geometric scaffolds. These are not possible using conventional methods [88]. Among the previously listed techniques, only a limited number have been used with frequency to produce scaffolds with controlled drug delivery characteristics. Three of the most used techniques are electrospinning, solvent casting, and freeze-drying. The following topics describe the specifics about the necessary conditions required for each of those methods in details, as well as the characteristics of the final devices. Also, the most recent 3DP are discussed as important novel approaches in solid polymer scaffold preparations.

4.1.1. Electrospinning

Electrospinning is the most widely used technique to fabricate ultrafine fiber-based scaffolds. The diameter of each fiber ranges from submicrons to a few nanometers, depending on the polymer specificity and processing parameters [89]. Since the time it was developed by Cooley and Morton in the early twentieth century, the technique has gained space and popularity among researchers due to its simplicity, ability for application with several polymers, cost-effectiveness, and its potential to scale up [90,91]. The technique can be separated in two categories. They are referred to as solution electrospinning (Fig. 3A) and melt electrospinning (Fig. 3B). While solution electrospinning uses a solvent to solubilize the polymer, melt electrospinning employs a heat system at the instrumental apparatus to provide a polymer in a liquid state at the absence of solvent [92]. Currently, solution electrospinning is responsible for approximately 90 percent of the fabricated ultrafine-based scaffolds. However, melt electrospinning is a viable alternative when there is no appropriate solvent to dissolve the polymer, or when traces of toxic solvents exist that are undesirable for some biological applications [92,93]. Another advantage of melt electrospinning is the higher stability of the melt polymer jet compared to the polymer solution jet. This is due to its higher viscosity that prevents repulsive Coulombic charge interactions. This allows for better control of fiber deposition compared to the randomized method from solution electrospinning [93]. Also, melt electrospinning has produced smoother nanofibers and less porous structures than solution electrospinning. This is useful to decrease the drug release rate in most cases[94].

The fundamental concepts of electrospinning are similar in both solution and melt methods. The ultrafine fibers are produced when the polymer melt or polymer solution is extruded through a needle of a syringe using a syringe pump under the presence of a strong electric field (up to tens of kV). The fiber is deposited on a regular or cylinder surface that is maintained at an optimal distance from the needle. In solution electrospinning, when a difference of potential is applied between the needle and the collector, charges tend to accumulate on the liquid droplet of the needle. At a sufficiently high voltage, the Coulombic repulsion overcomes the surface tension of the polymer solution and an electrically charged jet is ejected from the needle into

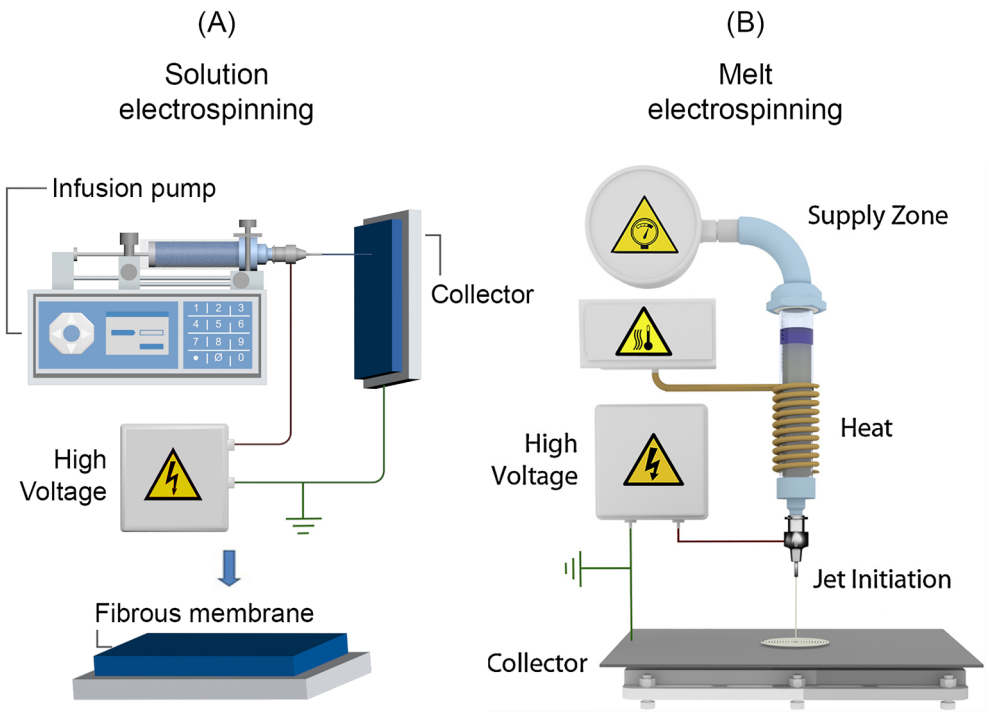

Fig. 3. Illustration of (A) solvent electrospinning and (B) melt electrospinning. Fig. 3B was reprinted from Ref. [93] with the permission of Elsevier. (Reprinted from Progress in Polymer Science, Vol 56, Authors Toby D. Brown, Paul D. Dalton, and Dietmar W. Hutmacher, Title of article Melt electrospinning today: An opportune time for an emerging polymer process, Pages No. 116–166, Copyright (2016), with permission from Elsevier.)

the collector. Before achieving the collector surface , the solvent is vaporized as a function of its volatility at the operating temperature. The solid polymer fibers are then deposited. For melt electrospinning, the extruded polymer solidifies and forms the fibers.

Both methodologies allow for the creation of single or multiple membrane layers by successive depositions (Fig. 3). This is useful to produce multilayers that load different drugs [95], which permits the physical separation of incompatible drugs or provides different drug release rates of several drugs by changing the characteristics of each layer. In practical terms, a variety of parameters can affect the drug release and the formation of fiber, including the applied voltage, needle diameter, and distance between the needle and the collector. These parameters must be optimized. A complete description of each parameter is described in previous reviews in the literature [96,97].

Electrospun scaffolds have been recently used in drug release to improve therapeutic efficacy and prevent postoperative adhesions [98]. Other regenerative medicines [99] for bone regeneration [100], wound healing [101], endothelialization acceleration, and lumen stenosis prevention [54] have been explored. Due to their large mesh size, electrospun membranes are permeable to gaseous and biological fluids. This allows a controlled drug release that accelerates the healing of the skin wound [102]. In some cases, a less permeable matrix may be desired, which can be obtained from simple solvent casting.

4.1.2. Solvent casting

Solvent casting is one of the simplest techniques used to produce thin film-based scaffolds through solvent removal from a polymer solution confined in a mold. The methodology consists of solubilizing a polymer or a blend in a single or a mixture of solvents, transferring the solution to a suitable mold, and incubating it at a fixed temperature until complete solvent evaporation (Fig. 4A). Due to this simple protocol, the modulations of the characteristics of the scaffold are limited by the choice of the polymer and solvent, as well as the incubation condition that drives the solvent removal rate (such as humidity and temperature) [103–106]. Also, the molecular weight and degree of acetylation of the polymer play a role on the final characteristics of the scaffold [107].

Comparisons between solvent casting and electrospinning techniques have shown that electrospinning tends to produce thinner, smoother, and more folded scaffolds than solvent casting [108,109]. Also, a more uniform drug distribution and less residual solvent may be found with the eletrospun scaffolds than those produced by solvent casting. As a consequence, more well-controlled drug release profiles might be obtained from electrospinning [108].

The limitations of the conventional solvent casting technique hinder the design of highly porous scaffolds. Throughout therapy, porosity is an important factor when modulating the efflux and influx of molecules, nutrients, oxygen, and the drug. It enhances surface area-to-volume ratio, which increases the drug release rate. For this aim, the technique can be modified by adding salt particles in a derivation known as salt leaching.

4.1.3. Salt leaching

Salt leaching uses salt particles in polymer colloidal solution to act as porogens during the formation of the thin film (Fig. 4B). After solvent evaporation, the salt particles are distributed throughout the scaffold and can be removed by the addition of water that solubilizes the particles. After salt removal, their sites are presented as pores in the scaffold. The final result is a porous film that presents a higher SSA than the similar one prepared by conventional solvent scaffolds. In addition to salt particles, a number of species are used as porogens, such as glucose and ionic liquids [87,110].

The creation of porous scaffolds is advantageous for cell attachment and for enhancing drug loading and retention. However, the pores formed by salt leaching can be mainly distributed on the surface of the scaffolds as a result of the limited permeation of water through the inner parts of some 3D platforms. In these cases, the freeze-drying technique can be explored to achieve a more porous 3D dimension scaffold.

4.1.4. Freeze drying

Freeze-drying (lyophilization) is a method of the production of solid and simple 3D devices widely used in the pharmaceutical industry [112]. In this method, porous scaffolds of simple 3D geometries are fabricated by solvent removal using sublimation (Fig. 4C). In general terms, the polymer solution is casted onto a mold of a desired

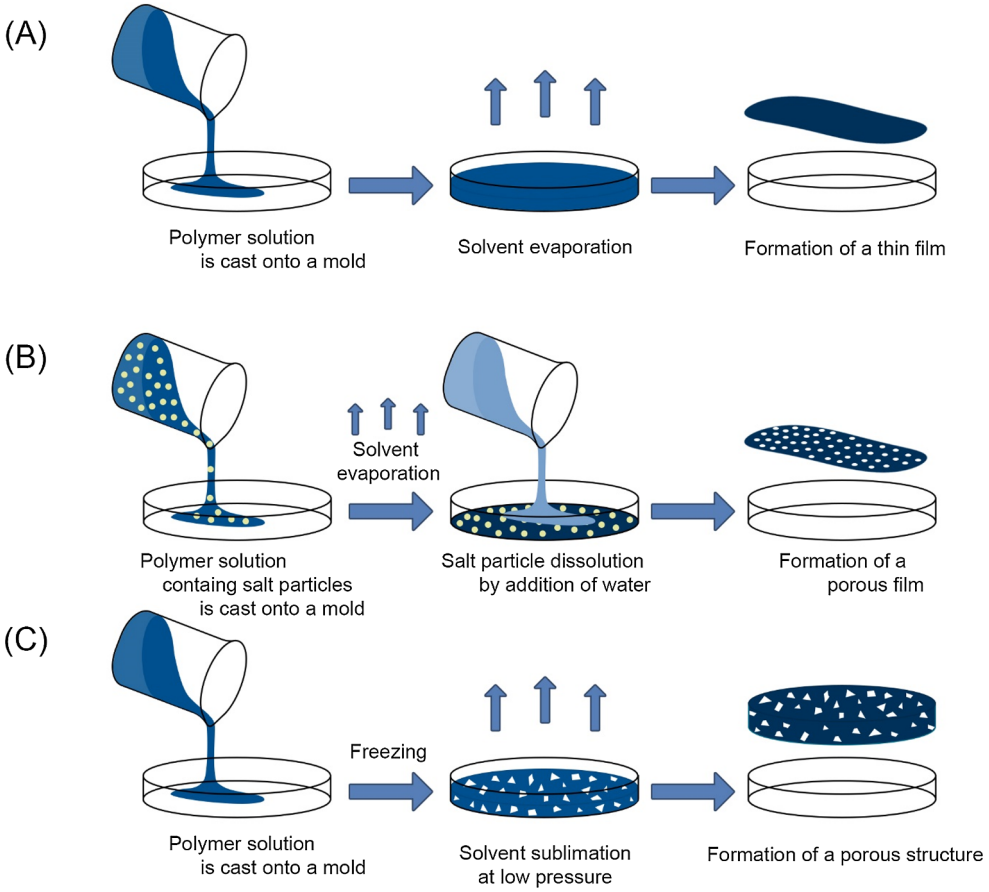

Fig. 4. A schematic illustration of (A) solvent casting, (B) salt leaching, and (C) freeze drying. Adapted from Ref. [111] with permission from The Royal Society of Chemistry.

dimension and kept at a temperature below its melt point for the period of time that is sufficient to freeze it. After that, the solvent is sublimed under a temperature below the glass transition temperature [113]. Generally, the same temperature that was used for freezing is recommended (using dryer equipment). Water is the most common solvent in freeze-drying. Although an aqueous medium is useful for water soluble polymers and drugs, the use of hydrophobic compounds can be limited. As an alternative, organic solvents or organic–water mixtures have been also used. In these cases, their freeze process can be challenging [113].

Freeze-drying can create porous 3D scaffolds, but their geometry is limited by the molds. Moreover, the method fails to create the most intricate networks. These are currently achieved using additive manufacturing (AM).

4.1.5. 3D printing

AM, also known as 3D printing, refers to the technologies that use computer-assisted deposition of materials to print physical 3D devices. The controlled layer-by-layer process makes AM the most current and versatile method to produce high quality polymer scaffolds. Moreover, design/computer-aided manufacturing (CAD/CAM) software enables the design of different geometries, a variety of networks, different pore sizes, multilayers, multicompartments, among others. This versatility has potential in the controlling of drug release rates. In addition, the unique possibility to convert computed tomography scans into computer models can generate 3D bioscaffolds, in other words, biologically functional scaffolds with the complexity and heterogeneity of tissues and organs. In these cases, a variety of active compounds (including growth factor) can be loaded to enhance desired biological responses.

Since 1986, the development of stereolithography [114] has led to a variety of novel 3D printing technology. This has been developed to enable the use of different materials. Descriptions of all 3D technologies is out of the scope of this review and can be obtained in detail from previous works [115].

For all the polymer implants, a prefabricated patient-specific geometry must be optimized. 3DP non-flexible scaffolds are likely not the most appropriate option for some biological applications that need geometrical adequation and more dynamic behavior, such as for the treatment of traumatic spinal cord injury and cartilage repair. In these cases, an injectable can be administered with minimal invasion. They can take the three-dimensional form of the application site before being gelled under an internal or external stimulus.

4.2. Injectable scaffolds

Most injectable scaffolds are hydrogels of a 3D network formed *in situ* by crosslinked hydrophilic polymer chains of a natural or synthetic origin that can swell in water or biological fluid and maintain their structures. Due to this particularity, hydrogels can retain a significant amount of water (greater than 70% water content) within the 3D network. This is because of the interaction between water molecules and hydrophilic groups of the polymer chains (such as −OH, −COOH, and −CONH−) and is followed by more hydrophobic interactions and osmotic force effects [116,117]. The hydration leads to some physical similarities between the hydrogels and the extracellular matrix. Along with their biocompatibility, these characteristics have led to the increase in research studies in the biomedical field concerning injectable scaffolds [118–120].

Hydrogels can be divided into two large classes (chemical and physical hydrogels) according to the nature of the crosslinking that

forms the polymer network. Essentially, chemically crosslinked hydrogels present a permanent network, but physical crosslinkings are reversible. More detailed classifications organize them into sub-groups, such as by the nature of the polymer, degradability, and the structure [121]. A complete description of the classes of polymers and methods of hydrogel preparation is not the aim of this review, but some attention will be given to the crosslinking that governs the methods of preparation and affects drug delivery profiles.

4.2.1. Chemical crosslinking

In chemical hydrogels, 3D networks are formed by polymer units linked by covalent bonds using a chemical crosslink agent or by photoprocesses (using UV radiation) [121]. In these reactions, functional groups (including OH, NH_2, and COOH) can form covalent linkage networks between polymers chains through reactions of these functional groups, with complementary reactivity (amine-carboxylic acid, isocyanate-OH/NH_2 reaction, or Schiff base formation) that conducts with hydrogel scaffold formations through crosslinking agents [122,123]. In the same respect, linkage networks can be achieved through Diels-Alder cycloaddition, addition chemistry through bis or higher functional crosslinking agents, and Michael addition. These involve thiol groups that are added to the activated α,β-unsaturated carbonyl polymers under basic reaction conditions [122,124,125]. Crosslinking agents applied in polymer reticulation include N,N-(3-dimethyl aminopropyl)-N-ethyl carbodiimide (EDC), hexamethylene diisocyanate (HMDI), poly(ethylene glycol) diglycidyl ether (epoxy), glutaraldehyde (GTA), genipin, glycidyl methacrylate GMA, and poly (ethylene glycol) diacrylate (PEGDA) [20,123,126,127].

4.2.1.1. Photopolymerization. Photo-induced crosslinking is related to the reaction of unsaturated groups. In most cases, (meth)acrylates are reactive when exposed to irradiation that incorporates to a polymer chain through a free radical crosslinking. Free radicals may attack near polymeric monomers or through their own double bond. This results in a crosslinked region [128]. Generally, polymer material that presents hydroxyl, carboxyl, and amino groups can react with acryloyl chloride, glycidyl methacrylate (GMA), and N-(3-aminopropyl) methacrylamide. These are responsible for the introduction of vinyl groups in the material [20].

4.2.1.2. Metal ion. Metal ion crosslinking is based on the coordination between metal cations and polymeric systems. The metal ion is responsible for linking linear polymeric chains that lead to a three-dimensional structure. The intermolecular interaction forces itself between metal cations. Polymeric ligands bring solid-state plasticity, excellent mechanical strength, and recyclability to the material [129].

4.2.1.3. Disulfide bridge. Crosslinking by disulfide bridges is currently used in self-healing hydrogels and hydrogels scaffolds that mimic biological gels [130]. The methodology preparation basically consists of mixing polymeric components and crosslinking solutions comprised of thiol groups (-SH). In general, applied thiol crosslinkers are monofunctional PEG-thiol (PEG-1SH), bifunctional PEG-thiol (PEG-2SH), 4-arm PEG-thiol (PEG-4SH), ethoxylated-trimethylolpropan tri(3-mercaptopropionate) (ETTMP), pentaerythritol tetra(3-mercaptopropionate) (PETMP), and pentaerythritol tetramercaptoacetate (PETMA) [130,131].

Despite their promise as effective methods, they can lead to HA hydrogels with large mesh sizes and highly hydrated structures. This can allow for the free diffusion of drugs of small molar masses. Moreover, low light penetration in human skin [132] may limit hydrogels from being formed *in situ* for such approaches. Finally, the use of toxic crosslinkers limits the application of a hydrogel-based injectable in biological tissue. In this scenario, physical crosslinking presents itself as a viable option to chemical crosslinking.

4.2.2. Physical crosslinking

Physically crosslinked hydrogels are characterized by physical domain junctions, such as hydrogen bonding and hydrophobic interaction [121]. Moreover, complementary associations of other lateral groups have been frequently used to structure a variety of self-healing hydrogels [133]. The next topics describe the most common physical crosslinking approaches to fabricate hydrogels that target drug release.

4.2.2.1. Hydrophobic interaction. Block copolymers that contain at least one hydrophilic and one hydrophobic moiety are generally thermoresponsive. Above a critical temperature (known as the upper critical solution temperature, or UCST), these copolymers are soluble in all ranges of concentration. Similarly, they are soluble below a lower critical point (lower critical solution temperature, or LCST). Between these points, the system can coalesce in a concentration-dependent manner. Thus, in some conditions, the copolymers present a thermoreversible sol-gel transition. This occurs due to the dependence of solubility of at least one moiety with the temperature. As an example, the degree of hydration of poly(propylene oxide) (PPO) increases as the temperature decreases. Pluronic® triblock copolymers that are comprised of PEO and PPO units present higher solubility at low temperatures, but tend to aggregate as the temperature increases. This forms hydrogels of some percentage in water. Pluronic F127, a common copolymer for the fabrication of hydrogels of physical sol-gel transition, presents an LCST from 25 °C to 37 °C depending on its concentration [134].

4.2.2.2. Shear-thinning and self-healing. For medical purposes, the absence of cytotoxic promoters of crosslinking is desired. Some of the current alternatives to initiator-mediated crosslinking is based on some well-established designs of hydrophobic association-based hydrogels [135], as discussed earlier. Systems of complementary associations have been used in a class of hydrogels to target crosslinked structures. These are known as shear-thinning and self-healing hydrogels. Pairs of complementary associations that are used for such purposes include those based on cucurbit[n]urils [136], pillar[n]arenes [137], and calix [n]arenes [138]. The pairs are covalently bound throughout to distinct polymer chains to confer such properties.

The self-healing process involves a physical-chemistry interaction between a guest molecule and a macrocyclic host cavitand. They are both laterally bound on distinct polymer backbones, as illustrated in Fig. 5. When blended in water, complementary associations are formed. They keep the polymer chains crosslinked. This forms hydrogel. Under high pressure conditions (in most cases $<$ 1 kPa [139]), the host-guest interaction is disrupted (shear-thinning property), which frees the polymer chains. This leads to low viscosity in the system. Such behavior allows the system to be injectable. This injection flows through a syringe, as the pressure is imposed on the colloid during the injection. After administration, the imposed pressure is quenched, and the host-guest interaction is reconstructed (self-healing property). This forms a guest-host hydrogel. To increase hydrogel moduli of such soft hydrogels, as well as their *in vivo* stability, a secondary crosslinking can be provided after injection by a second crosslinking reaction that forms a dual-crosslinking hydrogel [140]. This is important for various applications, including the limiting of left ventricular remodeling in infarcted myocardium.

In myocardium infarct, affixed patches and wraps have been used as restraints to stabilize the infarct planar expansion [141]. Targeting a minimally invasive percutaneous delivery, Rodell et al. (2016) fabricated a self-healing hydrogel to a percutaneous intramyocardial injection to act as a restraint. They provided the functionalization of a HA-based backbone with either β-cyclodextrin (β-CD), the host cavitand, or adamantane (Ad) to act as a guest molecule yielding CD-HA and Ad-HA polymers. A number of host-guest hydrogels have shown promise in clinical trials with intramyocardial injections. Despite the lack of mechanical stabilization and rapid degradation, the authors demonstrated

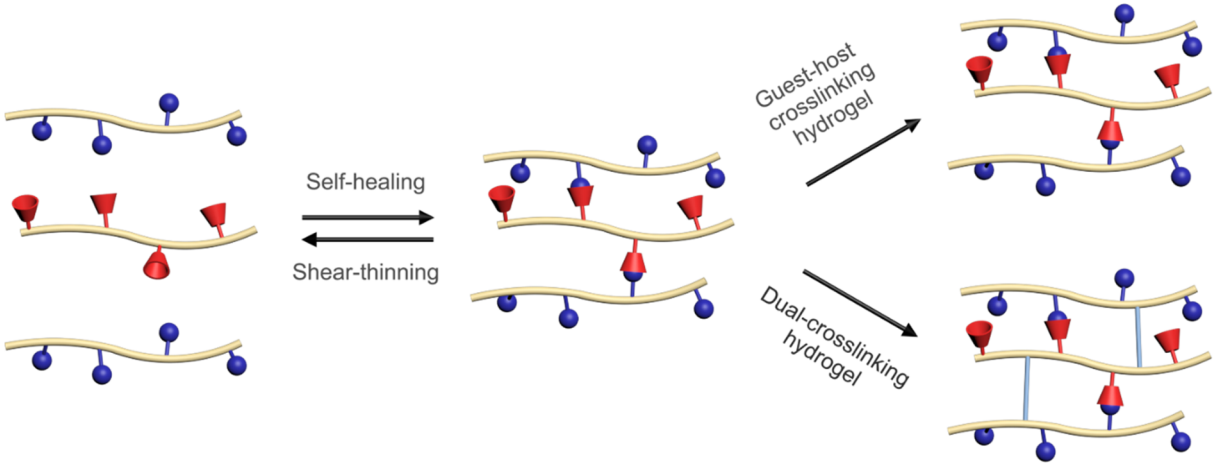

Fig. 5. Illustration of the process of shear-thinning and self-healing forming hydrogels with single host-guest crosslinking or dual host-guest plus chemical crosslinking.

that an *in vivo* dual crosslinking exhibited a suitable moduli (30.3 ± 2.6 kPa) and maintained the dual-crosslinked hydrogel stable for eight weeks (5.1 ± 0.2% degradation) [139]. Through DDS in animal models with myocardium infarct, host-guest hydrogels have been used to release growth factors that provided cardiac repair, enhanced cardiac function, and angiogenesis [142–146]. In addition, the release of anti-inflammatory agents by these hydrogels has shown promise for myocardial infarction[147] and kidney injury treatments [148].

Other shear-thinning and self-healing hydrogels with mild reaction conditions and high reaction rates have been designed based on Schiff-based linkages. Such bases may be obtained through the reaction of aldehyde groups along macromolecular chains with amino, carboxyethyl, or hydroxyl groups disposed into other polymer chains. Schiff-based hydrogels have been rapidly prepared (< 60 s) by mixing synthesized dibenzaldehyde-terminated poly(ethylene glycol) (DF-PEG) with glycol-chitosan at 20 °C [149]. In saline solution, this chitosan-PEG hydrogel showed an initial burst with 33% of Taxol released for up to two days and a slow release of 50% at day seven. *In vivo* intra-tumor injections in female nude mice (Fig. 6A) provided almost complete remission after 18 days of the injection of taxol-loaded self-healing hydrogel (Fig. 6B). This showed better results compared to a black solution, a Taxol solution (positive control), and a taxol-loaded non-self healing F127 hydrogel injected with the same methodology [150].

The same hydrogel has been used for other purposes, including the delivering of antihemorrhagic carbazochrome to target embolization therapy [151] and incubating stem cells for cell therapy [152]. Similar approaches have also been explored to design self-healing hydrogels to release doxorubicin [153], DNA [153], and nanoparticle-loaded drugs [38,154].

Despite the proposed single use of these platforms, hydrogels with Schiff-bases have also recently been tested as drug-reloadable depots. A recent study designed an alginate/chitosan-based hydrogel that was able to sequentially reload carbon quantum dots. These scavenge reactive oxygen species from inflammation sites [155]. The authors have highlighted that this approach can be useful in avoiding multiple

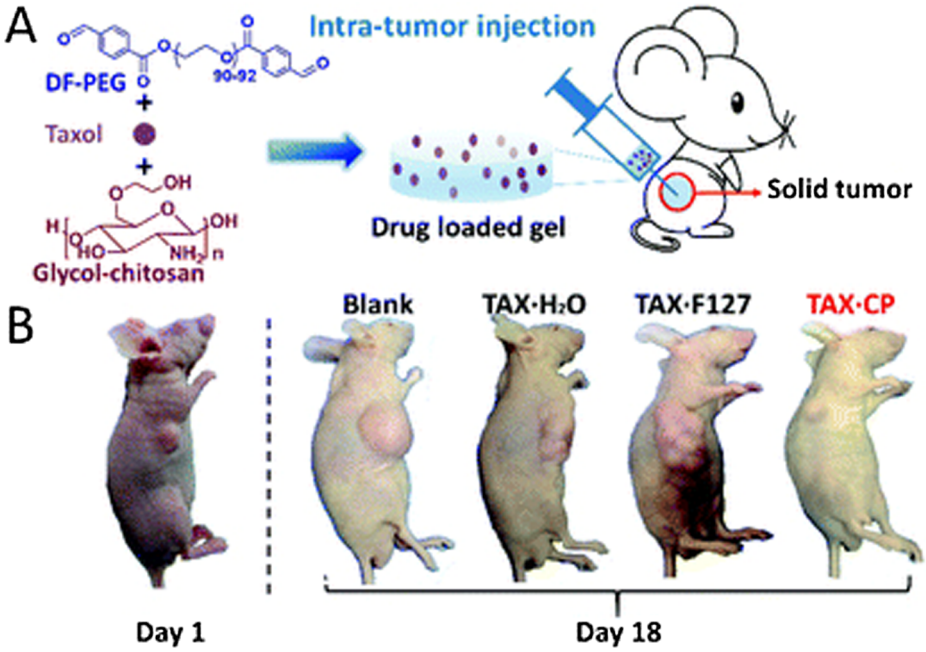

Fig. 6. (A) Illustration of the intra-tumor injection of the hydrogels. (B) Images of nude mice at day one and from the four different treatments on day 18. Adapted from Ref. [150] with permission from The Royal Society of Chemistry.

rounds of surgical implantation when the repeated local administration of drugs is required. It could also facilitate the loading of different drugs for polymer scaffolds.

5. Methods of drug-encapsulation

The load of drugs in polymer scaffolds can occur during or after their fabrication by a variety of techniques. The most common approaches involve a previous blend of the polymer and the drug, soaking the free-drug scaffold into drug solution, site-specific binding of the drug to the polymer, pre-loading in nano/microparticles, and drug-polymer conjugation. The selection of a method depends on the polymer-drug compatibility, the preparation method of the scaffold, drug stability, the final application, and the desired drug release rate. The following topics detail current methods of drug loading, differences between them, and their final effects.

5.1. Blend loading

The most commonly used strategy for obtaining a final drug-loaded polymer scaffold is based on the blend of the polymers and drugs before the fabrication of the platform. This allows for the drug to be incorporated during the formation of the scaffold. To blend them, the simplest way is by mixing solutions of the polymer and the previously prepared drug in a common solvent. Variations are common and generally match with the needs of the scaffold fabrication method. For example, the insertion of crosslink agents into the drug solution is performed when the beginning of the polymer network formation is at a desirable level. To obtain free-solvent mixtures, polymers containing the drug can be melted. This strategy is most used in hot-melt extrusion to produce drug-loaded filaments for 3DP. However, melt polymers may also be attractive as alternatives to prevent the use of cytotoxic solvents.

Except in cases of specific binding or drug-polymer conjugation, the distribution and phase state of the drug in the scaffolds depend on the physical-chemical interaction between the drug and polymer. The drug–polymer miscibility can be predicted by rational strategies using mathematical models based on parameters of solubility [156]. Their use is encouraged as a primary tool for screening drug/polymer blends. This is used to decide the drug load strategy for a specific pair of polymers and drugs. With respect to physically favorable interactions, the blending strategy generally yields a soluble and highly homogeneous distribution of drugs inside the matrix. The drug is embedded in polymer blocks or formed filaments. Thus, the favorable interaction tends to allow acceptably high levels of drug loading. Conversely, physically unfavorable interactions stimulate some phase segregation of the drug and polymer. This favors a heterogeneous distribution with the majority of the drug located at the surface of the scaffolds [157]. In critical cases, a complete segregation and formation of crystal on the surface of the scaffold occurs [157]. Thus, an unfavorable interaction decreases the drug loading efficiency.

The major limitation of the strategies based on blending is the use of a common solvent. For unfavorable interactions, a common solvent can be rare. Examples include the use of an organic solvent to solubilize hydrophobic synthetic polymers and water-soluble actives, such as proteins [158]. Poor solubility of drugs in the solvent during fabrication of the scaffold also leads to drug crystallization inside the polymer matrix. In these cases, the use of melt approaches has provided amorphous states for the drug loading scaffold [94]. Unfortunately, strategies of melt polymers can be difficult for thermo-sensitive drugs [159]. Strategies of drug loading after the fabrication of the scaffold (known as soak loading) can contour such difficulties.

5.2. Soak loading

Soak loading allows for drugs to be embedded in a pre-fabricated drug-free scaffold. This strategy consists in submerging the scaffold in a solution of the drug until its loading. Various factors play a role on the efficiency of soaking, including the drug/hydrogel mesh size, scaffold porosity, scaffold free volume, and wettability of the matrix. As an example, in PLA-based 3DP, the presence of micropores enhanced the loading of ampicillin and cytochrome *C* by approximately five and 10-fold, respectively, compared to the non-microporous prints [52].

In the case of hydrogels, the mesh size plays a role on the soaking load of the actives. The mesh size of hydrogels generally ranges from 5 nm to approximately 100 nm. This is high enough to allow for the influx of a variety of small compounds. On the contrary, the mesh can create a steric hindering for macromolecules typically larger than 40 kDa [126,160,161], including some proteins or drug-loaded nano/microparticles. This steric hindering limits the partition of some macromolecules to the shell region, decreasing the drug loading efficiency.

Similar to what occurs in the blend strategy, the force of interaction between the drug and the polymer plays a role on modulating the drug loading from the soaking load. In this method, unfavorable drug-matrix interactions create an environment where the drug is poorly embedded, and its use is discouraged in most cases [162]. This limitation can be contoured by strategies of site-specific binding of the drug to the polymer.

5.3. Site-specific binding

Polymers that hold functional groups with affinity to drugs allow for the site-specific binding of the drug to the polymer backbone. A rational approach for complementary associations can enable a homogeneous condition and a stronger drug-polymer interaction. As the number of specific sites can vary, the efficiency of loading depends on their total amount.

In addition, functional groups at the polymer backbone involve aminolysis, hydrolysis, reduction, and oxidation, among others [163]. For example, an aminolysis reaction yielded free amino groups on the PCL scaffold. Due to these groups, 2-N, 6-O-sulfated chitosan (26SCS) was immobilized in the scaffold after soak loading for four hours. As a result, the loading of 26SCS at the PCL fibrous scaffold was enhanced up to 100 times when compared to the unmodified PCL scaffold. Also serving as a site of binding, 26SCS enhanced the load of the BMP-2 growth factor when compared to the non-functionalized PCL scaffold [162].

5.4. Drug-polymer conjugation

Unfavorable drug-polymer interaction can also be solved by the conjugation of the drug to the polymer in a covalent manner. This strategy has an advantage over drug-loaded nano/microparticles, as it allows for precise control of the quantity of the incorporated drug. Also, it is suitable for providing strong stability of the drug in the matrix, preventing drug aggregation, quenching the burst release, and avoiding drug loss at later stages of sterilization or purification of the scaffold, such as in the removing of crosslink agents. Moreover, drug conjugation efficiently decreases the release rates of drugs when compared to physical loading approaches [164]. Finally, drug-polymer conjugation is a smart strategy to increase the loading of drugs in a highly efficient manner [165].

The most common chemical conjugations of drugs and polymers involve coupling reactions through esterification, amidation, and oxidation [166]. Esterification occurs between alcohol (hydroxyl (−OH)) and carboxil (−COOH) groups of the polymer and the drug. For example, when using coupling agents (such as N,N′-dicyclohexylcarbodiimide, known as DCC), the carboxil group of the drugs can react with the OH− terminal of the polymers, including PEG and PPO [167]. Carboxyl groups can also be conjugated to amine groups in a reaction of amidation when catalyzed by n-hydroxysuccinimide (NHS) or EDC [166].

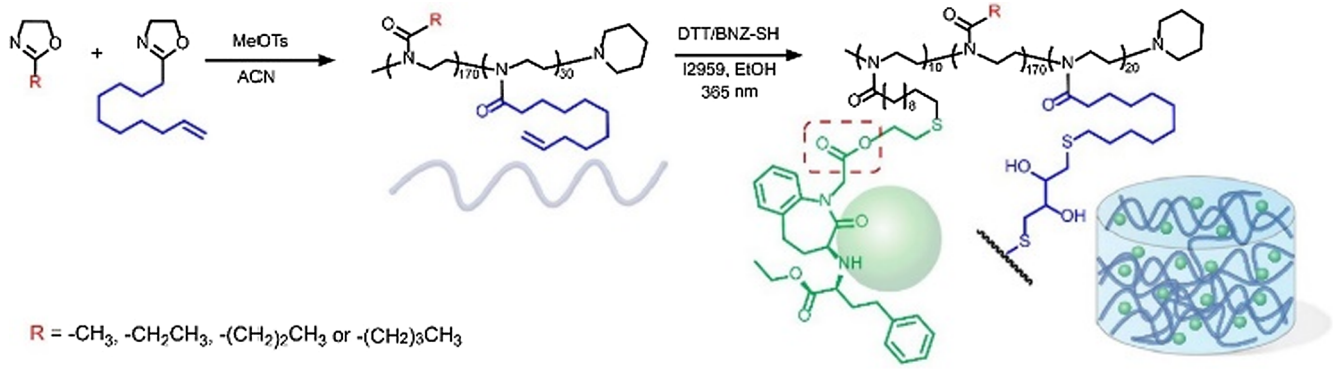

Fig. 7. Synthesis of copolymers and the conjugation of the drug benazepril using a biodegradable spacer as a well-located cleavage point for the drug release. Reprinted from Ref. [164] with the permission of Elsevier. (Reprinted from European Polymer Journal, Vol 120, Authors Jong-Ryul Park, Joachim F.R. Van Guyse, Annelore Podevyn, Eleonore C.L. Bolle, Nathalie Bock, Erik Linde, Mathew Celina, Richard Hoogenboom, and Tim R. Dargaville, Title of article Influence of side-chain length on long-term release kinetics from poly(2-oxazoline)-drug conjugate networks, Pages No. 1–9, Copyright (2019), with permission from Elsevier.)

Some drug-polymer conjugations are described in the current literature, including cefuroxime to chitosan [168], ibuprofen to PEG [167], and HIF-1 conjugated with polyacetal [169]. In a recent study, Parket et al. (2019) added a thiol group to benazepril and used it to conjugate to a homologous series of synthetized polymers by thiol-ene photo-conjugation, as illustrated in Fig. 7 [164]. These drug-conjugated polymers were used to prepare hydrogels. They suggested that increasing hydrophilic polymer moieties enhanced release rates.

Frequently, a labile linkage is used between the drug and polymer as a biodegradable spacer (as indicated by the traced square in Fig. 7) to yield a well-located cleavage point for drug release.

5.5. Pre-loading in nano/microparticles

Another alternative to unfavorable drug-polymer interaction is pre-loading the drug into nano/microparticles before embedding into scaffolds [87]. This is also useful to contour the lack of a common solvent in the blending strategy. The method consists of loading the drug in small polymer particles, and then confining it within the scaffold polymer networks during pre-[170] or post- fabrication [171]. In pre-fabrication, generally the polymer is first homogenized in an adequate solvent, and then the particles are added under stirring until complete dispersion. In this technique, the solvent must be inert in the particle, ensuring the maintenance of its structure. In post-fabrication, the free-drug scaffold is soaked in a solution of drug-loaded particles similar to what is described in the Soak Loading topic [171].

A summary of the drug encapsulation modes in polymer scaffolds is shown as a flowchart in Fig. 8. The classes of drug loading and their main influences on drug release are discussed in the following topics. They are summarized in Table 1.

6. Drug release

The kinetics of drug delivery from polymer scaffolds is essentially governed by desorption, dissolution, and diffusion of the drugs, as well as erosion, swelling, and degradation of the matrix. In some cases, desorption and diffusion of the most interfacial molecules leads to an initial burst [172]. The bulk drug, however, can depend on all the factors related to the drug and polymer network. The mechanisms of the drug release rates can be tuned by the methods of drug encapsulation, the nature of the polymer, the method of the scaffold preparation, the degree of the network of the scaffold, multiple layers, and porous structures, among others. Due to the variety of factors, polymer scaffolds can yield a series of bursted, controlled, and sustained/zero-order drug release profiles, and even pulsatile and biphasic profiles. A rational approach on the mechanisms that govern the drug delivery can be supported by a variety of mathematical models, including Hixson–Crowell and Korsmeyer–Peppas models [172–176]. In the following topics, the factors that affect the drug release from scaffolds are discussed, as well as a number of current strategies employed to modulate them.

6.1. Free volume of implants

The release of the drug can be limited to the interface of non-biodegradable scaffolds. This includes their pores, as the drug molecules located in the core of the polymer matrix cannot be desorbed [177]. Thus, the free volume of solid implants can control the bulk drug release. High free volumes make the scaffold permeable to water molecules, allowing drug desorption and diffusion. As free volume decreases, steric hindering rises and creates drawbacks to the dynamic of water and drug efflux. For example, higher release rates for drugs such as Quinine (from the PCL scaffold) compared to a PLLA-based one were explained by the differences of their permeabilities [178]. Another effect of free volume is the limiting of drug diffusion by steric hindering. With respect to the drug, steric hindering increases as the drug size increases. Thus, drugs with higher sizes tend to show slower or even more quenched release rates when compared to smaller ones [179].

6.2. Mesh size of hydrogels

The mesh size of hydrogels can also limit the drug release of some actives. In fact, this is one of the most important factors to regulate the diffusion of actives inside hydrogels [180]. It can prevent the diffusion-based release of macromolecules, mainly those larger than 40 kDa [126,160,161] or drug-loaded nano/microparticles. In these cases, further processes of relaxation of the polymer chains and their biodegradation can govern the release rate if the diameter of the drug is around or slightly higher than the mesh size. In the case of relaxation processes, the wettability of the scaffold can favor conformational changes on the polymer network allowing the diffusion of these drugs. Strategies to modulate the release rate involves changes of the concentration of the polymer and/or crosslink agent to alter the mesh size of hydrogels [181]. Drugs that are considerably larger than the mesh size are expected to have erosion-controlled releases.

The roles of the degree of interconnectivity from host-guest interaction in shear-thinning and self-healing hydrogels are similar [81]. In general, the amount of host-guest interactions between the polymer chains is limited by a random distribution of functional groups throughout the polymer backbone. This decreases the number of effective associations between host and guest units among polymer backbones. As a consequence, the mesh size created can be too high to inhibit macromolecule diffusion. To contour this, hydrogels of geometric favorable host-guest interactions have been obtained. For this

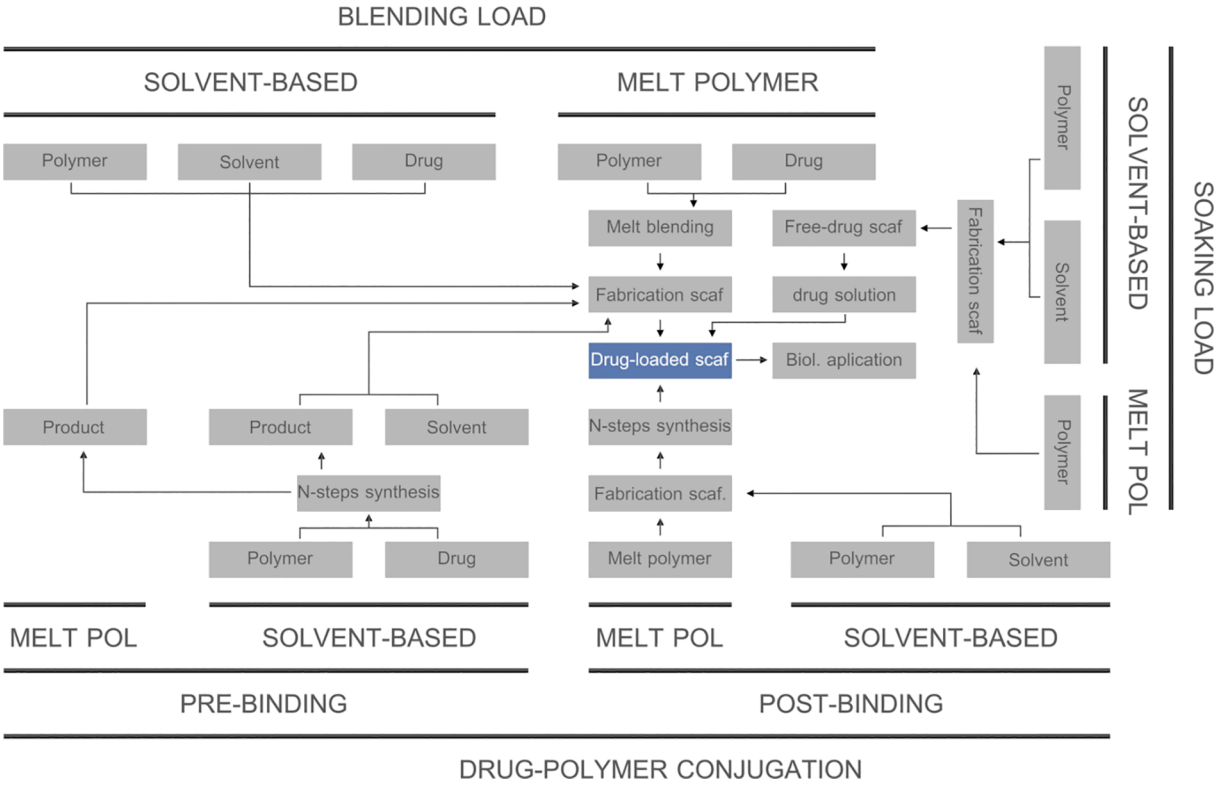

Fig. 8. Flowchat of methods of drug-loaded scaffolds preparation.

purpose, host–guest pairs are formed before the photopolymerization of the polymer backbone [182]. During the polymerization, the pairs are linked. This yields favorable complementary geometry after the polymer is formed. To target such conditions, a study used iso-cyanatoethyl-acrylate-modified β-CD as the host unit and 2-(2-(2-(2-(adamantyl-1-oxy)ethoxy)ethoxy)ethoxy) ethanol acrylate as the guest unit [182]. After complexion in the reaction media, the polymerization of the lateral groups provided the polymer backbones with well-orientated host-guest interactions. Such an approach prevented steric-hindrance, optimized the host–guest inclusion, and created highly crosslinked hydrogels [182]. This strategy may allow erosion-controlled delivery of a number of proteins, antibodies, DNA, and siRNA from these modified hydrogels.

The polymer mesh can not only limit the efflux, as suggested earlier, but also the influx of macromolecules [183]. This property has controlled reaction-diffusion degradation mechanisms, such as those mediated by enzyme [183] that may modulate the drug release of macromolecules. Moreover, adjusting the polymer mesh shows

Table 1
General methods of drug encapsulation and their most common influence on drug release.

Type	Drug-matrix interaction	Common drug-loading capacity[a]	Drug distribution into matrix	Common behavior of drug Release	Main factors that affect the drug release
Blending	Physically favourable	High	Homogeneous	Sustained/controlled	Physical-chemistry drug-matrix interaction; Degree of crosslink; Wettability; Surface area-to-volume ratio; Degradation of matrix; Drug size
	Physically unfavorable	Low to Medium	Heterogeneous	Initial burst release	
	Site-specific	High[b]	Heterogeneous	Sustained/controlled	Degree of crosslink; Wettability; Surface area-to-volume ratio; Force of interaction; Degradation of matrix
Soaking-load	Physically favorable	Medium to high	Heterogeneous[d]	Controlled	Physical-chemistry drug-matrix interaction; Degradation of matrix
	Physically unfavorable	Low	Homogeneous[d]	Burst/rapid release	Force of interaction; Degradation of matrix
	Site-specific	High[b]	Heterogeneous	Controlled	
Drug-polymer conjugation	Covalent	High[c]	Heterogeneous	On-demand/slow and extended drug release	Cleavage of spacer; Degradation of matrix

[a] Metric relative to the efficiency of the other polymer scaffolds.
[b] Variable as a function of number of active sites per unit of surface area.
[c] Simply tuned by adjusting the number of reactive sites in the polymer backbone.

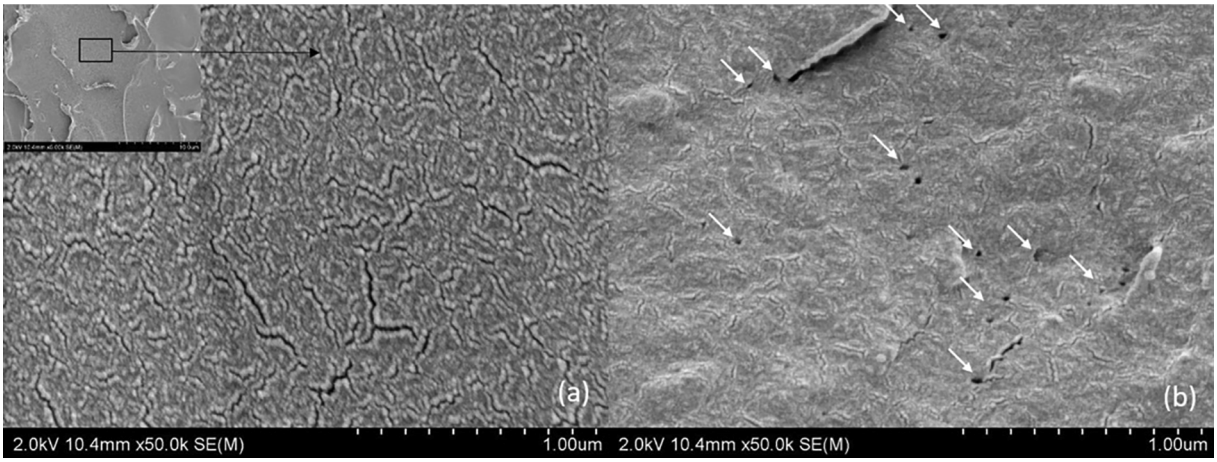

Fig. 9. SEM cross section images of PLA scaffold (A) before and (B) after drug release. Reprinted from Ref. [184] with the permission of Elsevier. (Reprinted from International Journal of Pharmaceutics, Vol 548, Authors Jingjunjiao Long, Ashveen V. Nand, Sudip Ray, Sam Mayhew, David White, Craig R. Bunt, Ali Seyfoddin, Title of article Development of customised 3D printed biodegradable projectile for administrating extended-release contraceptive to wildlife, Pages No. 349–356, Copyright (2018), with permission from Elsevier.)

potential in the matching of the matrix degradation kinetic with the rate of tissue regeneration [126].

6.3. Drug-matrix interaction

6.3.1. Physical interaction

Polymer and drug molecules can interact at physical and chemical levels by the van der Waals interactions, hydrogen bonds, electrostatic interactions, and covalent bonds, among others. With respect to unfavorable drug-matrix interactions, an intensified initial burst release is common as a result of the more interfacial distribution of the drug in the scaffolds, as well as the crystalline phases of the drugs in the scaffold. The crystalline phases can also be a result of poor drug solubility in the solvent that is used to fabricate the drug-loaded scaffold, as discussed earlier. The solubilization of these aggregates in physiological mediums creates pores at the scaffold surface (Fig. 9) [184]. These pores intensify the bulk drug release due to enhancement in the water infiltration within the scaffolds. This bursts the drug release.

Conversely, stronger physical or specific interactions yield lower drug release rates [185]. Thus, adding functional groups of association with the drug on the polymer backbone is a smart strategy to decrease the release rate of actives. As an example, drugs that present high affinities to hosts (such as β-CD) can have their release controlled by inclusion complexes [186]. Joshua et al. (2015) evaluated the affinity of molecules for β-CD-HA using L-tryptophan as a drug model [186]. Non-significant association was observed using unmodified HA. Conversely, L-tryptophan exhibited high affinity to β-CD-HA with an association constant (K_a) of $1.6 \times 10^4 \pm 2.9 \times 10^3\ M^{-1}$ to HA functionalized (around 35%) with β-CD. As a result, the mobility of a peptide containing tryptophan residue, GKWEWKWE-FITC (3 W), decreased in the bulk of the hydrogel as the β-CD content increased. When the tryptophan residue was removed, the diffusion of 3 W significantly increased. The authors demonstrated that the cumulative release after 24 h decreased from 90% to 20%, while changing from unmodified to functionalized HA. A similar β-CD effect was even observed for doxorubucin and doxycycline, being more pronounced for doxycycline due to its higher affinity for β-CD [186]. On the same principle, the release of compounds that present affinity to β-CD (including imazalil [187], curcumin [188], resveratrol [189], α-mangostin [190], carvacrol [191], olsalazine [192], camptothecin [193], and caffeic acids [194]) could be modulated with a similar strategy. With the same objective, other specific interactions have been explored, such as BMP-2/sulfonated chitosan [162].

Most of the blends discussed above have yields that busted, controlled, or sustained the drug release profile. Conversely, some diseases need an on-demand release. This is typically due to processes of temporal physiological changes. For this reason, nonuniform drug delivery can be preferred instead of continuous ones in some cases.

6.3.2. Chemical interaction

Biodegradable spacers that link drugs to polymers allow for a well-located cleavage for drug releases that are free of polymer residues. In these cases, the drug release rate is controlled by the kinetics of the cleavage of such groups. Moreover, these groups enable the possibility of drug release in a responsive way to enzymes, redox species, pH, and light, among others. In the case of *in vitro* drug release, Parka et al. (2019) demonstrated that the cleavage at the ester spacer was responsible for a quicker release when catalyzed in a basic medium compared to the neutral aqueous solution.

In the absence of a biodegradable spacer or when the cleavage of the spacer is not facilitated in physiological media, the release of drugs may be governed by the degradation of the matrix [195]. Thus, the drug release rate will be a function of the nature of the polymer, which can occur over several years. As an example, the PCL presents a slow degradation rate of around two to three years before being excreted through urine and feces (without cumulating in organs) [196]. A variety of products can be used in these cases, such as conjugated drug-oligomers [165]. A detailed understanding of these products is needed for the control of adverse drug effects, including *in vivo* cytotoxicity.

To summarize the discussion above, Fig. 10 shows the factors that affect the drug release from polymer hydrogels. As described previously, most of the concepts are also valid with other polymer scaffolds forms. Beyond these variables, a number of other modifications of the polymer units can be used to tune the release rate, as well as to trigger the release by biological or external factors. Moreover, changing a range of characteristics of the scaffolds (such as SSA and biodegradability) can be used to tune the release rates of the drugs. The following topics describe a number of current strategies employed for modulating drug release rates by polymer scaffolds.

7. Modulating the drug release

7.1. Polymer blends

Without chemical functionalization, the optimization of the desired release profile and drug solubility can become difficult in systems with unique backbone polymer-types, despite the variety of polymers currently employed in scaffolds for drug delivery. Thus, polymer blends are

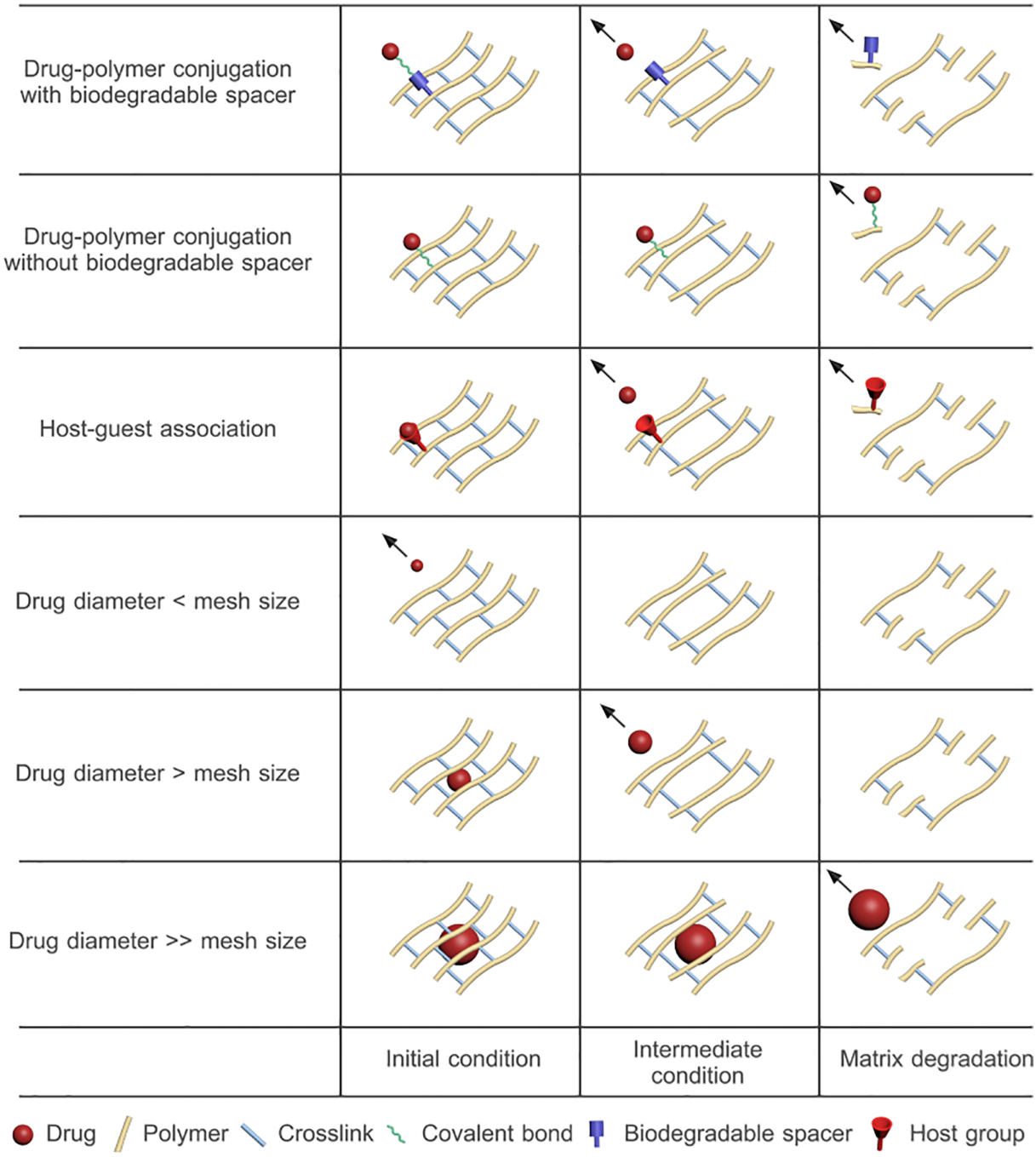

Fig. 10. Illustration of drug release modes by hydrogels at different drug sizes and drug-polymer interactions.

convenient physical modifications to mix the properties of different polymers (in ideal mixtures) or even to generate novel properties (in non-ideal mixtures) [197,198]. Simple binary polymer blends are common in the fabrication of scaffolds and possible for some compatible pairs of polymers within a range of proportion. Ternary blends are also used [198], but with less frequency. This is because they may exhibit more complex phase separations [199]. These separations can create drawbacks for their use in some conditions. To avoid experimental complications, previous evaluations of the miscibility of the polymers using mathematical theories (such as Hansen's solubility parameters) are encouraged [200].

As a miscible binary mixture, hydrophobic-hydrophobic polymer blends are simple and smart strategies for modulating erosion-based drug delivery. This is useful to allow for the controlled release of macromolecules that cannot diffuse throughout the polymer matrix. Moreover, this strategy can tune the scaffold biodegradation with the finite time of therapy, avoiding a second surgical intervention to remove it. In these cases, it is important that their biomechanical integrity supports the new tissue, especially in the early stages of growth. They need to present a kinetic of degradation aligned to the rate of tissue regeneration, with complete dissolution and absorption by the body at the time of the cure. If a concomitant specific drug delivery profile is desired, this optimal degradation rate should be modulated in an attempt to align with both the regeneration rate and drug release kinetic. One smart approach of hydrophobic blends is to use compatible synthetic polymers, such as PLA, PGA, PLGA, and PCL that present different degradation rates. As an example, the PLGA content increased the degradation rate of electrospun PCL/PLGA, as well as promoted cell

infiltration *in vivo* [201].

Compatible hydrophilic-hydrophobic polymer blends can optimize the drug release and improve the drug-matrix compatibility. Drug release rates can be enhanced as the hydrophilic fraction increases in these blends. The electrospun compatible Chitosan/PMMA blends yielded a sustained release of ciprofloxacin as a function of chitosan content, in other words, the hydrophilicity of the scaffold [177]. Interestingly, the hydrophilic polymer also plays a role on the dissolution rate of poor water-soluble drugs in blends. The blends are more efficient than simple hydrophobic scaffolds because of the hydrogen bonding between the drugs and the hydrophilic polymers [202].

Incompatible hydrophilic-hydrophobic polymer blends lead to pore-forming scaffolds. Low fractions of the hydrophilic polymer segregate themselves into several nuclei throughout a hydrophobic polymer matrix. In physiological media, they can be hydrated and/or solubilized. This allows for the water influx, which enhances desorption and the release of the drug. The role of hydrophilic polymers into hydrophobic scaffolds was evaluated using electrospun examples comprised of PEO/PMMA (10% PEO) and PVA/PMMA (< 15% PVA) throughout the loading of ciprofloxacin [177]. For PEO/PMMA, their incompatibility segregated them into the nucleus of PEO throughout the PMMA matrix. In the physiological medium, the PEO was leaching, creating pores, and bursting the drug release. Thus, approximately 70% of ciprofloxacin was released in the first day. As PEO and PMMA did not form a homogeneous matrix, the remaining ciprofloxacin was embedded in the PMMA phase and was not released even after 17 days. PVA also yielded a burst release of ciprofloxacin, but the release was different than the PEO/PMMA blend. With PVA, there was a complete release as a result of the better miscibility of the polymers. Also, the lower solubility of PVA in water compared to PEO led to a more controlled release of over 17 days.

Targeting to optimize mechanical properties and the toughness of the final product, a variety of polymer blends have been explored [203]. Optimization processes have also been used to improve the printability of polymer inks in 3DP, as well as to modulate their drug release [204]. Conversely, blends are inefficient in providing an on-demand release, typically due to the lack of sensitivity to external agents. However, a variety of treatments can benefit from nonuniform drug delivery rather than a continuous one.

7.2. Responsive polymer scaffolds

The on-demand release can be obtained by using responsive polymer scaffolds. They are platforms of drugs or cell releases controlled by biological or external stimuli known as triggers [205]. The most common biological triggers are local pHs, oxidation–reduction endogenous agents, and enzymes. Ultrasound, light, and the magnetic fields constitute the most common external triggers used to date. Currently, there are a number of polymers that are intrinsically responsive to such stimuli. Moreover, stimuli-sensitive structures can emerge even in non-responsive polymers, typically through a variety of blends with stimuli-sensitive nanoparticles, surface modifications of pre-formed scaffolds (including crosslinking with thermoresponsive moieties), and coated approaches. In the next topics, some of the most current scaffold applications for responsive or on-demand drug release systems will be explored.

7.2.1. Internally triggered

7.2.1.1. pH. Though the development of rapid-response scaffolds under biological triggers is challenging, functionalized polymers hold great promise concerning sensitivity to internal stimuli. Anna and Katarina (2018) have employed palladium-catalyzed oxidative carbonylation to develop pH-responsive hydrogels [206,207]. This imine-functionalized chitosan–palladium macrogel provided a pH-controlled pulsed release of fluorescein in homogeneous media. Based on chemical oscillators, an oscillatory mode of the diffusion-governed release of fluorescein was observed, which was fully matched with oscillations of pH [206]. Such a system may even be applied in cancer treatment due to the fact that the tumor microenvironment is frequently more acidic than in normal tissue. Another characteristic of neoplastic tissue is their higher levels of reactive oxygen species (ROS). This feature can be explored as a biological trigger for the on-demand release of anti-cancer drugs in the neoplastic environment.

7.2.1.2. Reactive oxygen species. ROS are oxygen-based species present in the cellular environment. They serve as indirect modulators of cell signaling pathways and homeostasis, typically due to their reactivity under normal and physiological conditions. Examples of biologically relevant ROS are hydrogen (H•), hydrogen peroxide (H_2O_2), singlet oxygen ($^1O_2$), hydroxyl (HO•), organic peroxides (ROOH), superoxide ($O_2^{\cdot -}$), peroxyls ($RO_2^{\cdot}$), peroxynitrite ($ONOO^-$), and Alkoxyl ($RO^{\cdot}$) [208]. In the biological context, the ROS level is regulated by a number of enzymes and antioxidants. The imbalance between ROS and the cellular antioxidant factors results in structural damage in normal cells, commonly known as oxidative stress. Conversely, malignant tissue takes advantage of the oxidative milieu to promote tumor progression.

Targeting ROS-responsive scaffold, Wang et al. (2018) designed an PVA-TSPBA (N1-(4-boronobenzyl)-N3-(4-boronophenyl)-N1,N1,N3,N3-tetramethylpropane-1,3-diaminium) scaffold loading gemcitabine and anti–PD-L1 blocking antibody (aPDL1) [209]. The ROS-labile linker TSPBA was synthesized through the quaternization reaction of N1,N1,N3,N3-tetramethylpropane-1,3-diamine in the presence of 4-(bromomethyl)phenylboronic acid. The PVA-TSPBA crosslink network was quickly obtained by a simple mixture process, typically through the spontaneous meeting of two phenylboronic acids from TSPBA with diol groups of PVA. In aqueous solution at 37 °C, the scaffold showed a higher delivery rate (than in neutral condition) of gemcitabine and aPDL1 in the presence of 1.0 mM of H_2O_2, which pointed to some degradability stimulated by ROS. In healthy mice, the self-healing structure was completely degraded after approximately 21 days. Against tumor-induced mice, tumor regression was reported to both 4 T1 breast tumors and B16F10 melanoma at a low PD-L1 expression cell line (Fig. 11).

Gupta et al. (2014) synthesized an ROS-sensitive polymer of architecture triblock ABC comprising poly-[(propylenesulfide)-block non-self-healing-(N,N-dimethylacrylamide)-block-(N-isopropylacrylamide)] (PPS-b-PDMA-b-PNIPAAm) [210]. Because of the thermoresponsivity of PNIPAAm, it was possible to inject a PPS-b-PDMA-b-PNIPAAm polymer solution *in vivo* to form *in situ* physical hydrogels. The injectable can reduce the local inflammation due to the ROS-scavenging properties of such a polymer [209]. This provides cell-protective action against oxidative stress.

7.2.1.3. Reducing agent. Glutathione (GSH) is a reducing agent abundant in almost all animal cells. With respect to cancer, the elevated levels of glutathione play a protective role and create resistance to a number of chemotherapeutic drugs [211,212]. New polymers have been designed for sensitivity to glutathione to act as triggers for drug release. Diblock PCLDMA-BACy (Poly(ε-caprolactone) dimethacrylate-bisacryloylcystamine) gels of different PCLDMA/BACy ratios were soaked with levofloxacin, a drug of small molar mass (Mw = 370 Da). In PBS, the levofloxacin release rate showed an initial burst followed by a slower phase, with a cumulative release of less than 20% after approximately 30 days. Conversely, the presence of glutathione led to the release of more than 80% after approximately 120 h, being more pronounced to the gel with greater BACy content. This study suggested that the presence of glutathione *in situ* can trigger the drug release from such gels [213]. Glutathione-mediated hydrogel degradation has also been obtained through covalent disulfide crosslinks, because there is cleavage via the reaction of reduction. They have been used for on-demand releases of chemotherapy drugs [214], proteins [215], living cells [216], or to generate degradation

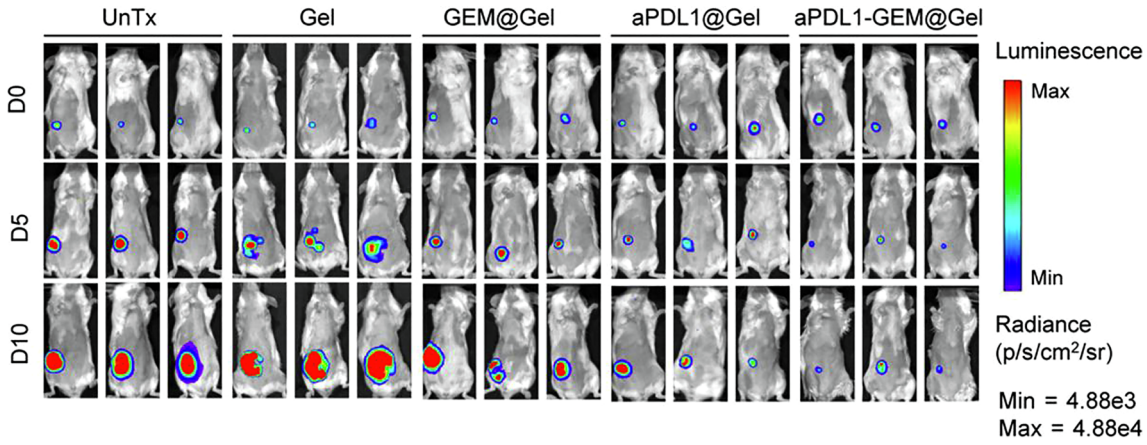

Fig. 11. *In vivo* bioluminescence imaging of the B16F10 tumor within three representative mice in control and treated groups with local gel scaffold loading of different active compounds. Reproduced from Ref. [209] with permission from American Association for the Advancement of Science.

products of antioxidant properties [217].

7.2.2. Externally trigged release

7.2.2.1. Temperature. Another way to control the drug release is to use thermoresponsive polymers. These compounds can be explored to cover the pores of the scaffolds in temperatures above their LCST, hindering the diffusion of the loaded drug. Using this strategy, the thermoresponsive capacities of scaffolds comprised of chitosan, collagen, and their blended scaffolds have been achieved by crosslinking glutaraldehyde followed by coating with poly(*N,N′*-diethylacrylamide) (PDEAAm). This exhibits an LCST between 32 °C and 35 °C [22]. This causes a change from a more hydrophilic character in an expanded coil conformation below the LCST to a higher hydrophobic compact globule conformation above the LCST, such as body temperature. As a proof-of-concept of temperature-mediated release, ibuprofen presented a staircase profile of cumulative release for cycles of temperature exchange between 25 °C and 37 °C. This system seems to be even more attractive in controlling the delivery of molecules of high molar masses due to a better control of diffusion throughout the hydrogel layers, as demonstrated using bovine serum albumin [218].

The on-demand release by temperature may need to be optimized for the LCST of polymers through chemical modifications. Adding hydrophilic moieties, the LCST enhances but lowers as the hydrophobicity of the moiety increases. The polymer PNIPAm exhibits an LCST of approximately 32 °C, as previously mentioned [219]. Wang et al. (2013) have copolymerized NIPAAm monomers with both hydrophilic acrylamide (AAm) and graphene oxide (GO), which led to a PNIPAAm (97.5%)-PAAm(2.5%)-GO hydrogel with an LCST of 39.0 °C [220]. The thermoresponsive hydrogel was used to efficiently capture human umbilical vein endothelial cells and provide cell releases triggered by near-infrared light in a reversible manner. On the contrary, the addition of more hydrophobic moieties into the PNIPAAm structure decreased LCST values. As an example, Gan et al. (2016) recently designed a PNIPAAm structure linked to the hydrophobic PCLDMA and hydrophilic BACy moieties at different PCLDMA/BACy ratios [213]. The LCST of the PNIPAm-co-PCLDMA-co-BACy copolymers was shown to decrease with an increase in PCLDMA. Other PNIPAm-based scaffolds have been used for cell alignment [221], osteogenic differentiation [222], wound healing [223], and bone regeneration [224].

7.2.2.2. Light-induced temperature. To increase local temperature and achieve the LCST of the PNIPAm, magnetic nanoparticles can be used as triggers [225]. Such nanoparticles can promote local heating under irradiation by surface plasmon effects. Specific production methods can provide nanoparticles that absorb in a range of wavelengths with high tissue transition capacity. This is needed for biological applications. Beyond a phase transition effect, when combined, scaffolds loading magnetic nanoparticles can suffer physical collapse under irradiation. This led to the on-demand release of vancomycin (an antibiotic) from gold-based nanoparticles-loaded PNIPAm scaffolds resulting in efficient inhibition of *staphylococcus epidermidis* [226]. Such an approach could be explored to provide local on-demand delivery of a variety of antibiotics and other drugs.

7.2.2.3. Electric. Polypyrrole (PPy) is a conducting polymer that is useful for electrical devices and clinical applications. This is due to its biocompatibility and ease for polymerization. PPy electrically deposited above a polymethylmethacrylate template provides a porous PPy thin film with electrically stimulated drug delivery properties. Although a passive and sustained release profile was present, the active delivery of dexamethasone (a corticosteroid/anti-inflammatory drug) was significantly trigged by the application of + 0.6 V or –0.6 V and 0.5 Hz, with a staircase profile of cumulative release following several on-off electrical cycles [227].

7.2.2.4. Ultrasound. Ultrasound is the best provider of high spatial precision of drug deposition into the desired tissue by trigger approaches [228]. The propagation of ultrasound waves throughout the body can lead to variations in local pressure, cavitation, acoustic fluid streaming, and local hyperthermia [228]. For such effects, the application of the ultrasound alone has been consolidated as an efficient strategy to enhance drug penetration or cellular uptake mediated by a resulting effect known as sonoporation [229,230]. Its mechanical and thermal effects over DDS have been explored to provide localized drug release [228]. The effects of ultrasounds were evaluated over the release of fluorescein from a PLGA hydrogel. For this purpose, approximately 50 mg of PLGA/NMP hydrogel-loading fluorescein were directly injected into tissue-mimicking poly(acrylamide) gel phantoms as drug models. When treated with 2.2 W/cm^2 (for 10 min each day), the phantom exhibited a greater distribution of fluorescein when compared with the control, especially from day two to day 10. The evaluation of the fluorescence of fluorescein (near 0.2 cm from the center of the implants) showed intensity increases of 2.4, 6.0, 2.0, and 1.7-fold compared with the control after days three, five, seven, and 10, respectively. In addition, hydrogels under 0.7 W/cm^2 or heated at 42 °C did not show significant differences against the control [231].

8. Applications

Drug delivery polymer scaffolds have been studied against a range of diseases. These include (but are not limited to) cancer,

Table 2
Experimental trials with drug delivery polymer scaffolds.

Drug/drug model	Main scaffold Composition	Applications	Scaffold-fabrication Method	Drug-encapsulation method	Some *in vitro/vivo* experimental trials[f]	
Ciprofloxacin	Polydioxanone	Microbial infections	Electrospinning	Blending	*In vitro* using an infected human dentin *Enterococcus faecalis* biofilm model	[236]
Vancomycin	(n-isopropylacrylamide)-co-acrylamide, gold nanorods	Coating on biomaterials, e.g., osseointegrated implants for local drug delivery	Spin-coating	Soaking load	*In vitro* on-demand release of the antibiotic agent induced by NIR light in a *Staphylococcus epidermidis* culture: zone inhibition.	[226]
Paclitaxel and Vascular endothelial growth factor (VEGF)	Poly-L-lactic acid[i]	Intracranial aneurysms	Electrospinning	PTX: pre-loading nanoparticle VEGF: soaking load targeting surface site-specific binding	*In vitro* cytotoxicity analysis in human umbilical vein endothelial cells and human vascular smooth muscle cells, *in vivo* animals and vein pouch aneurysm model establishment, *in vivo* stent implantation	[54]
Ampicillin	Polycaprolactone, polyvinylpyrrolidone	Dental applications	Electrospinning	Blending	*In vitro* zone inhibition of a selected oral strain of *Streptococcus sanguinis*.	[237]
Doxorubicin	Poly(ethylene glycol) methyl ether methacrylate	Cancer	Photopolimerization	Covalent bond	*In vitro* cytotoxicity against MDA-MB-231 human breast cancer cells	[238]
Ibuprofen	Chitosan, collagen, poly(N,N′-diethylacrylamide)	pH- and thermo-controlled pulsatile release of bioactive molecules	Freeze drying, chemical cross-link, coating in supercritical media	Blending	-[b]	[218]
Docetaxel and Dexamethasone-acetate	Polycaprolactone-dimethacrylate, poly(ethylene glycol) dimethacrylate, poly(ethylene glycol) methyl ether methacrylate, methyl ether methacrylate, 2-hydroxyethyl methacrylate, n-propyl methacrylate, and their moiety combinations.	Drug-delivery devices for personalized medicine	Continuous liquid interface production	Blending	Cytotoxicity of any leachable or degradation product against HUVEC and HeLa cells.	[239]
Daptomycin, Polymyxin B, Tobramycin, Vancomycin, Caspofungin, Amphotericin B	Gelatin	Life-threatening burn-related injuries/infections	Electrospinning	Blending/covalent bond	*In vitro* biocompatibility assessment using primary human dermal fibroblasts; *in vivo* wound healing against burns on juvenile large white Yorkshire pigs	[195]
Cisplatin	Hyaluronic acid derivatives	Peritoneal dissemination of gastric cancer	Chemical crosslinking	Blending	*In vitro* cell proliferation assay toward MKN45P, a human gastric cancer cell line. *In vivo* experiments in a mouse model of peritoneal dissemination of gastric cancer	[37]
Levofloxacin	N-isopropyl acrylamide, poly (ε-caprolactone) dimethacrylate, bisacryloylcystamine	Tissue engineering scaffold applications	Polymerization	Soaking load	-[b]	[213]
Salvianic acid	Gelatin, polyurethane[a]	Vascular tissue engineering	Electrospinning	Pre-loading in nanoparticles	*In vitro* hemocompatibility, *in vivo* implantation in rabbit carotid artery	[98]
Carbamazepine	Acrylonitrile butadiene styrene	Anti-epileptic drugs	Fused deposition modeling	Drug powder packed into each scaffold	-[b]	[240]
5-aminolevulinic acid	Poly(methyl vinyl ether-alt-maleic acid), poly(methyl vinyl ether-alt-maleic ethyl monoester)	Photodynamic therapy	Electrospinning	Blending	*In vitro* cytotoxicity against HaCaT and SW480 cell lines	[241]
Clotrimazole	Polycaprolactone[c]	Antifungal scaffolds	Melt co-extrusion	Blending	*In vitro* antifungal activity against *Aspergillus fumigatus*, *Candida albicans*, and *Trichophyton*	[242]

(*continued on next page*)

Table 2 (*continued*)

Drug/drug model	Main scaffold Composition	Applications	Scaffold-fabrication Method	Drug-encapsulation method	Some *in vitro/vivo* experimental trials[f]	
					mentagrophytes, *in vivo* study using a mouse model	
Resveratrol	Poly(lactide-co-glycolide)	Adipose tissue inflammation	Pelleted, salt porogen-based, and gas-foamed[d]	Pre-loading in microparticles	*In vivo* implant into adipose tissue of mice	[243]
Paclitaxel, doxorubicin	F127, hyaluronic acid[e]	Solid tumor	Spontaneous transition sol–gel	pre-loading in nanoparticles/blending	*Ex vivo* determination of injectability	[38]
Doxorubicin	Hyaluronic acid-based[g]	Drug delivery vehicle	Self-healing	Pre-loading in nanoparticles	*In vitro* against human breast cancer cells	[154]
Dexamethasone	Polymethylmethacrylate	Electro-stimuli responsive implants targeting corticosteroid treatment	Electrodeposition	Blending	–[b]	[227]
Meloxicam, mitomycin-C	Polycaprolactone, chitosan	Inhibiting epidural adhesion post-laminectomy	Electrospinning	Blending	*In vitro* cytotoxicity and proliferation, *in vivo* in a rabbit laminectomy model	[244]
Miconazole	Chitosan, carbopol, gelatin, gum arabic, and alginate	Oral candidiasis	Solvent casting	Blending	*In vitro* mucoadhesive strength, *in vitro* Halo zone test against *Candida albicans, C. glabrata, C. tropicalis, C. parapsilosis, C. krusei.*	[103]
Cefazolin	Polycaprolactone	Tissue regeneration preventing complications from bacterial infection	Fused deposition modeling and salt leaching	Drug solution drop-loading	*In vitro* cytotoxicity against 3 T3 fibroblasts, *in vitro* antibiotic bioactivity testing against *S. aureus*, *in vitro* blood clot formation	[245]
Gemcitabine, anti–PD-L1 blocking antibody	Poly(vinyl alcohol) (PVA) with an ROS-labile linker: N1-(4-boronobenzyl)-N3-(4-boronophenyl)-N1,N1,N3,N3-tetramethylpropane-1,3-diaminium	Localized chemoimmunotherapy	Spontaneous *in situ* hydrogel formation	Blending	*In vitro* B16F10 and 4 T1 cancer cells studies. *In vivo* gel formation and degradation in healthy mice, *in vivo* release pattern in the B16F10 mouse model, *in vivo* response of immune cells and tumor cells after treatment, *in vivo* Scaffold-mediated combination therapy against B16F10 mouse melanoma tumor model, B16F10 incomplete tumor resection model, and 4 T1 tumor model of triple-negative breast cancer.	[209]
Metronidazole	Polycaprolactone, gelatin[h]	Therapeutic applications requiring time-extended functions	Electrospinning	Pre-loading in nanotubes	*In vitro* antibacterial activity against *Fusobacterium*; *in vitro* cytotoxicity using L929 fibroblast cells.	[246]
Taxol	Chitosan-based	Tumor chemotherapy, drug delivery system	Self-healing hydrogel	Blending	*In vivo* toxicity and therapeutic effect against human hepatocarcinoma tumor into female nude mice	[150]

[a] Loading salvianic acid-loaded mesoporous silica nanoparticles.
[b] Release studies in homogeneous or microheterogeneous media.
[c] Poly(ethylene oxide) is present at the preparation step.
[d] The particular procedure is well described in material and methods of the reference (Murphy et al., 2018).
[e] Paclitaxel was previous loaded into micelles composed of Pluronic F127 and α-tocopheryl polyethylene glycol 1000 succinate.
[f] *In vitro* studies refer to all studies that have used cell lines; release studies in homogenous and microheterogeneous media were not considered as *in vitro* studies.
[g] DOX-loaded nanoparticles were loaded into the HA scaffold.
[h] Drug-loaded halloysite clay nanotubes doped into polycaprolactone/gelatin microfibers.
[i] PTX-loaded mesoporous silica nanoparticles within electrospun polylactic acid fibers with immobilized VEGF.

cardiovascular diseases, arthritis, Alzheimer's disease, and epilepsy. A variety of them are listed in Table 2. Also, the evolution of the production of polymer scaffolds for use in the pharmaceutical field has exhibited much promise in the control of the release of a broad spectrum of active compounds with antimicrobial, antifungal, and anti-inflammatory properties, as well as in the delivery of osteogenic and angiogenic factors in regenerative medicine. This will be described in the following topics.

8.1. Antimicrobial scaffolds

Despite advances in medical procedure, post-surgery complications have occurred in some implants. Infections by opportunistic pathogens are one of the most common and dangerous complications associated with the use of implant devices, including polymer scaffolds. Among bacteria genus, *Staphylococcus* is the most frequently involved in orthopedic infection. *Pseudomonas*, *Enterococcus*, *Streptococcus*, and *Enterobacteriaceae family* have also been isolated from patients with such implants [232]. Such infections have emerged despite the advancement of the technology of medical devices. They currently correspond to 25.6% of healthcare-associated infections in the United States [233,234]. This is even more problematic in devices that remain for a long period of time in the body, such as long-term drug delivery scaffolds or prosthesis. Tissue infections cause failure of the devices along with chronic disease, and lead to the necessity for implant replacement. Sometimes, treatment difficulties are caused by antimicrobial resistance [235]. To avoid these complications or to target other therapies, a number of scaffolds can carry and deliver *in situ* antibiotics.

Antimicrobial agents interrupt the life cycle of a microorganism by either inhibiting its growth or its division mechanism and cell transport [247]. One of the most serious issues in such an approach is the presence of antibiotic resistance. This is caused by the adaptive response of microorganisms that become tolerant to a certain amount of drug that would normally be effective. Such an occurrence has frequently made a number of potent antibiotics completely obsolete [248,249].

Controlled drug delivery shows promise as a method to decrease the induction of antibiotic resistance mainly by decreasing the fluctuation of the drug level in the plasma. While targeting the controlled release of curcumin, a natural drug with high antimicrobial activity, Sedghi and Shaabani (2016) provided the first core-shell nanofiber-based membrane comprised of a polymer-free curcumin core and a PVA-chitosan shell by the coaxial spinneret electrospinning technique. Concerning the release of curcumin, they showed that the core/shell arrangement limited the initial burst release, enhancing the sustainability of curcumin by overcoming its short half-life when compared with that of blended nanofibers. Related to antimicrobial activity, the high efficacy of the core/shell arrangement was obtained against methicillin-resistant *Staphylococcus aureus* and *Staphylococcus epidermidis* [95], showing considerable promise in multidrug-resistant organism treatment.

An intricate membrane was developed by Xue et al. (2015). It was composed of halloysite nanotube-loaded PCL/gelatin microfibers, and it was used to load and release metronidazole in a controlled manner [246]. Metronidazole-loaded nanotubes of 50 nm and 600 nm of diameter and length, respectively, were aligned within the 400-nm diameter electrospun fibers, resulting in an extended release (> 20 days) of metronidazole when compared to traditional PCL/gelatin microfibers (four days). The controlled release of the drug prevented anaerobic Fusobacteria colonization but permitted eukaryotic cell adhesion and proliferation throughout the following days. Another interesting electrospun scaffold was synthesized by incorporating thermally exfoliated graphene oxide (TEGO) as an antimicrobial agent into a three-dimensional fluorinated pentablock poly(L-lactide-*co*-e-caprolactone)-based scaffold [250]. The authors specifically addressed the significance of the surface-oxygen functional groups in the antimicrobial properties of graphene sheets. Results demonstrated that the thermal treatment of GO (with a low density of oxygen), affected the original graphene antimicrobial properties and inhibited antimicrobial activity *in vitro*. This was important in identifying bacterial growth inhibition conditions related to surface composition in graphene antimicrobial scaffolds.

Another important application of polymer scaffolds for antimicrobial purposes involves dressings for burn injuries, considering that this type of injury is highly exposed to infections, specifically those caused by antibiotic resistant bacteria. A recent study synthesized and evaluated dopamine-loaded electrospun gelatin nanofibers. Increasing dopamine concentrations seemed to increase the diameter of the fibers and promote intermolecular interaction, whereas the crosslinking after-treatment with $(NH_4)_2CO_3$ did not affect biocompatibility. A matrix with 2% pDA (polydopamine) was loaded with polyhydroxy antimicrobials to promote hydrogen bonding interactions and the controlled release of the drug. A weak inhibitory effect was only observed against Gram-positive strains. Kinetic release results indicated that a complete retention of antimicrobial activity was achieved for more than 20 days at a relatively low concentration of the drug (0.5% w/w). Based on these findings, a wound-dressing prototype was created incorporating vancomycin into the gel pDA mats, and its efficacy was tested using an animal model that simulated the pathophysiology of burn wounds in humans. Burn wounds treated with this prototype displayed higher keratinization and increased wound closure when compared with untreated wounds. This suggested a decrease in the number of inflammatory cells, an increase in fluid absorption during the early stages of healing, and an enhanced re-epithelialization rate [195].

Other studies have explored the antibacterial activity of drugs released by fibers, including the activity of ampicillin-loaded PCL nanofibers against *Streptococcus sanguinis* [237], ciprofloxacin-loaded polydioxanone nanofibers against *Enterococcus faecalis* [236], levofloxacin-loaded PCL-based nanofibers against *S. aureus and E. coli* [251], and pure polymer-based fibers, such as chitosan with NHS groups immobilized on PCL fibers [252].

8.2. Antifungal scaffolds

Similar to bacteria, antifungal approaches have received the attention of researchers of polymer scaffold-based materials in the last few years. Against oral candidiasis (the most common opportunistic infection in the human immunodeficiency virus), polymer scaffolds have advantages when compared to approved tablets or gel, as they are more flexible, less removed by saliva, and offer protection for the wounded mucosa [103]. Tejada et al. (2017) produced miconazole nitrate-loaded polymer films composed of chitosan, carbopol, gelatin, gum arabic, and alginate. Among them, chitosan/carbopol-based and chitosan/gelatin-based scaffolds showed valuable mechanical properties and adhesiveness, as well as superior *in vitro* activity against the *Candida* genus, when compared with miconazole nitrate raw material. Another study using a clotrimazole-loaded melt co-extruded PCL-based fiber demonstrated *in vitro* extended antifungal activity in front of electrospun samples against Aspergillus fumigatus, Candida albicans, and Trichophyton mentagrophytes [242]. The antifungal activity of the scaffold was also demonstrated and compared to controls in a mouse model.

8.3. Anti-inflammatory scaffolds

Inflammation is a necessary process in human health, for example, in the early stages of the wound healing process. Acute inflammation indicates a physiological response that occurs in vascularized tissues to defend the host from pathogens, foreign bodies, injuries, and to maintain homeostasis. To stay healthy, both the initiation of acute inflammation and its resolution must be efficient. Otherwise, inflammation could be reduced by the use of external agents or drugs [253]. In a normal healing process, spinal laminectomy leads to epidural adhesion

formation with pain in the range of 5% to 30% of patients [254]. The early stage of laminectomy is responsible for a significant inflammatory reaction. Shi et al. (2019) have proposed the use of a double-layered electrospun nanofiber membrane based on PCL/chitosan blends to prevent epidural adhesion and reduce the inflammation reaction [244]. The layer was in contact with a vertebral-induced rabbit defect, with the inner layer loaded with meloxicam and a nonsteroidal anti-inflammatory drug to prevent an inflammatory reaction. The outer layer, in contact with fibroblasts, was loaded with mitomycin C, an anti-tumor antibiotic that has been used to prevent adhesion formation [255]. This dual system significantly reduced inflammation and prevented epidural adhesion formation in the rabbit model.

For anti-inflammatory applications, natural polymers represent an important class of biomaterials. They feature good biocompatibility, which may induce a low inflammatory response after implantation in the body. These biomaterials can be classified among those with anti-inflammatory properties or that serve as DDS for an anti-inflammatory agent [256]. In the first category (biomaterials with intrinsic anti-inflammatory properties), some polysaccharides are highlighted for their beneficial properties, such as chitosan and chitooligosaccharides (COS) [256]. COS showed anti-inflammatory action when tested in paw edema in mice, which increased with the molecular weight. This demonstrated that the COS effect was dependent on the dose and molecular weight [257]. Mechanisms of COS anti-inflammatory action have been studied based on their ROS-scavenging properties [258]. Similarly, HA hydrogels have been widely studied due to their anti-inflammatory nature, especially with regard to regeneration applied to burn wounds [256]. PEG and its nano-conjugated derivatives are also commonly used, safe, nonimmunogenic molecules with anti-inflammatory properties.

In addition to natural polymers, low-molecular-weight PEG may potentially play a role in the therapy of systemic inflammation and sepsis [24]. Other synthetic polymer scaffolds are developed as delivery systems incorporated with anti-inflammatory drugs. PLGA scaffolds have been reported with a variety of incorporated drugs. For instance, the incorporation of stromal cell-derived factor-1 alpha (SDF-1α) into PLGA scaffolds was reduced locally to improve both the tissue response and regenerative potential in mice [256]. Kim and colleagues (2018) fabricated scaffolds using $Mg(OH)_2$-incorporated PLGA copolymer (MH-PLGA) and tested the anti-inflammatory effect and renal regeneration potency in mouse kidneys, and compared it to the effect of PLGA alone [259]. The MH-PLGA scaffold group showed lower expression of pro-inflammatory and fibrotic factors, low immune cell infiltration, and significantly higher expression of anti-inflammatory factors and renal-differentiation-related genes when compared with the PLGA scaffold group. This indicates high renal regeneration potency. Murphy and colleagues (2018) investigated resveratrol delivery from porous PLGA scaffolds designed to integrate with adipose tissue [243]. Resveratrol also decreases inflammation associated with biomaterial implants in bone, cartilage, and vasculature. They concluded that resveratrol delivery from scaffolds can induce an anti-inflammatory response in pro-inflammatory environments, including adipocytes, revealing a promising therapeutic strategy for the treatment of adipose tissue inflammation that drives metabolic disease.

Zachman and colleagues (2013) proposed a promising approach for improving soft tissue regeneration (blood vessel and heart muscle) when inflammatory diseases, such as ischemic tissue fibrosis and atherosclerosis, limit the regeneration process [260]. Porous scaffolds were tuned to meet the requirements for soft tissue regeneration by employing tyrosine-derived combinatorial polymers with polyethylene glycol crosslinkers. Another approach was the use of the technique of substrate-anchored and degradation-sensitive coatings. Wu and colleagues (2015) studied anti-inflammatory biodegradable implant materials using PLA/hydroxyapatite as an implant material model loaded with an anti-inflammatory drug to suppress the local inflammation caused by the degradation of implant materials [261]. Other examples are the PLLA scaffold release of ibuprofen to decrease inflammatory responses and improve muscle regeneration, and dexamethasone-incorporated hydrogels that reduce the inflammatory response in lipopolysaccharide-stimulated primary mouse macrophages *in vitro*. Though potential delivery systems have been reported, only a few anti-inflammatory drug delivery materials are currently used in clinics. One of these is a system for sustained delivery of dexamethasone with promising results for edema and inflammation control [256].

8.4. Tissue repair scaffolds

Though advances have been made on the prevention of post-surgery complications through inflammation-mediation (as discussed above), the regeneration of complex tissues and organs remains an important scientific challenge. The use of various BMP-loaded scaffolds have shown to be an effective way of overcoming challenges in several types of bone regeneration processes (including spine fusions with INFUSE®). Such examples have stimulated research in the last few decades. Bone regeneration is a multifaceted process comprised of a temporospatial sequence of biological events that involve several signaling pathways and different cell types for bone and neovasculature formation [262]. In such processes, growth factors (GF) play an important role in information transfer between cells and their microenvironment in tissue engineering and regeneration, while angiogenic factors stimulate the formation of vasculature responsible for oxygen and nutrient transport into the new tissue. They are proteins and peptides, usually exhibiting short half-lives. They should be present above a certain concentration *in vivo*. Indeed, optimized release rates *in situ* have been demonstrated to be one of the most important factors for a successful bone regeneration outcome [263]. Therefore, the incorporation of GF into scaffolds of tunable releases is being explored to provide a background capable of accelerating tissue regeneration. It is important to know that the mechanical properties of scaffolds may be reduced as the drug release increases [264], which is a point that must be considered in some cases.

In regenerative medicine, polymer-based scaffolds have been explored to load and deliver GFs, including BMP-s and basic fibroblast growth factors (bFGF) [15,17]. The first polymer delivery system was developed by mixing the GFs in an albumin gel. Other synthetic hydrogel matrices include PVA and PEG [265]. Some studies have focused on techniques to improve the incorporation of GFs in delivery systems to increase effectiveness during tissue regeneration. One of these techniques consists of protein immobilization combined with nanomaterial carriers. A recent review paper (2017) evaluated the latest techniques in direct immobilization and relevant biomaterials used for GF loading and release, including synthetic polymers, albumin, polysaccharides, lipids, mesoporous silica-based nanoparticles (NPs), and polymer capsules [266]. They concluded that when delivering GFs to promote tissue regeneration, the most important factor is to obtain optimal concentrations and gradients of the suitable GF for precise spatial/temporal demand. Most of the evaluated delivery systems have demonstrated enhanced stability and therapeutic potential of the GF upon immobilization when compared with traditional regenerative medicine and DDS. Specifically, NP-based GF delivery systems have demonstrated several advantages due to their high surface area, nanostructures, and precise control of multiple proteins, which play pivotal roles in the regulation of cellular adhesion, proliferation, differentiation, and extracellular matrix production. A recent study fabricated a blend of alginate sulfate and PVA scaffolds. The blend was capable of delivering a heparin-like growth factor and transforming growth factor-beta1 (TGF-β1). Results demonstrated the binding and entrapment of TGF-β1 to the nanofibrous scaffolds to deliver growth factors in tissue engineering applications [267].

The extensive studies in these areas have led to the first FDA approval of collagen-implant-loading BMP-2 (Medtronic's INFUSE®) in 2002. Researchers have reported excellent fusion rates with the use of BMP-2 in posterior and anterior lumbar interbody fusion [268–270].

Despite the fact that INFUSE succeeded, the limited capacity of BMP-2 to provide proper scaffold-infiltrated vascularization in bone regeneration has hampered other successful scaffold-delivered BMP-2 outcomes. Some of these outcomes have led to fracturing, fibrous tissue formation, and/or necrose processes in some poorly vascularized transplants [271]. Moreover, some complications associated with the use of BMP-2 were reported. Cahill reported ectopic and heterotopic bone formation, vertebral osteolysis, graft migration and subsidence, and antibody formation against BMP-2 [272]. The intrinsic inflammatory action of BMP has led in some cases (11.3% incidence among 204 patients) to a clinical condition of postoperative lumbar radiculitis, without apparent dose dependence [273]. An overview of the complications concerning the use of BMP-2 was discussed by Tannoury et al. (2013) [274]. Moreover, *in vivo* sustained dual delivery of osteogenic factors BMP-2 and IGF-1 from polymer scaffolds, such as PLGA/hydroxyapatite scaffold, have exhibited less attractive synergic effects than those obtained in *in vitro* assays. This shows promising synergism related to ALP activity and production of Runx2, OCN, and OPN [275–277].

The combinations of GFs and angiogenic GFs, such as platelet-derived growth factor (PDGF) and vascular endothelial growth factor (VEGF), have been studied to achieve synergic effects *in vitro* and *in vivo* with different delivery rates [278–280]. In these strategies, a smart sequential delivery of angiogenic and osteogenic factors seems to be essential for expressive synergism. In the last few years, in an attempt to optimize each biological stage and develop an efficient implant for bone regeneration, some efforts have been made to design polymer scaffolds for programmed and sequential deliveries of angiogenic and osteogenic factors. Hydrogel and microsphere combinations are frequently used in these scaffolds. Several of these studies evaluated the sequential release of angiogenic factors followed by osteogenic factors (A/O) and osteogenic factors followed by angiogenic factors (O/A).

For the A/O sequence, Bayer et al. (2017) designed a porous three-dimensional scaffold to release PDGF with overlapping BMP-2 delivery after five days. For this purpose, an interconnected porous network into an alginate hydrogel support was provided by the insertion of microspheres comprised of PLGA and calcium phosphate. The alginate hydrogel and microsphere composition provided a suitable environment for the sequential release of PDGF followed by BMP-2. As a result, the dual scaffold was able to promote differentiation of human mesenchymal stem cells toward an osteoblast phenotype to increase cellular infiltration, as well as up-regulate the alkaline phosphatase (ALP) expression. Similarly, a dual system comprising BMP-2-loaded microspheres within VEGF-loaded gelatin hydrogel showed an initial 3D burst release of VEGF and a sustained release of BMP-2 for up to 56 days [281]. The results showed that VEGF synergistically enhanced ectopic bone formation in the presence of BMP-2, though VEGF was not efficient when used alone.

Interestingly, compared to BMP-2 alone, neither vascularization nor a bone formation synergistic effect was seen in the orthotopic defects. This showed a lack of efficiency in the A/O sequence used for orthotopic defects. A more recent study evaluated the effect of the sequential order of the release of GFs, A/O and O/A using BMP-2 and VEGF as osteogenic and angiogenic factors, respectively. The study states that O/A is more efficient in facilitating new bone formation of ectopic bone *in vivo* [282].

9. Conclusion and perspectives

This review showed that controlled drug delivery from polymer scaffolds has emerged and presented potential in the development of smart therapies with synergic effects on the regeneration of organ and tissue loss, as well as to treat illnesses, including cancer and cardiovascular diseases. In the initial screenings of novel scaffolds, most studies have focused on physiological media and the *in vitro* release of drugs and low molar mass compounds. In more advanced stages, several drugs have been incorporated onto implants and injectable polymer scaffolds, and their release kinetics have been evaluated *in vivo*. Conversely, the lack of more consistent tests *in vitro* and *in vivo* of the most current scaffolds has created drawbacks to a deeper knowledge of the drug release behavior in biological tissue. This hinders its advancement in clinical studies. Indeed, only a few results describe the drug delivery profile from polymer implants *in vivo*. Even less information is available concerning the effect of tissue specifications on the modulations of such kinetic profiles. This results in fewer advances in the design of patient-specific scaffolds of controlled delivery for personalized medicine. However, it continues to be a promising approach for the future.

This review also showed that injectable hydrogels are the most common form of scaffolds based on studies of local controlled drug delivery. The main challenge of an injectable is still related to achieving both optimal mechanical strength and biocompatibility [182]. Moreover, the attempt to optimize the mechanical property with high crosslinking efficiency has challenges concerning yields due to degradation. This has led to incomplete drug release. In our opinion, this has been the limiting point of hydrogels and has created drawbacks to successful clinical outcomes. The authors believe that the development of other forms of injectable hydrogels, such as forms based on self-healing approaches, is essential for overcoming the current barriers. This applies not only to tumor chemotherapy, but also in other biomedical research, such as controlled drug delivery of small molar mass compounds.

Finally, most of the promising findings are related to the novel polymer scaffolds of multi-species delivery, including co-delivery of osteogenic and angiogenic factors, as well as anti-inflammatory molecules and immunomodulators (such as antibodies, lentivirus, and nucleic acids). Considering osteogenic factors, such as BMP-2 in bone regeneration and frequent post-surgery complications, future studies should focus on safety and restrictions in order to decrease collateral effects. The authors believe that the scaffolds of the future will present efficient controls against the formation of bacterial films on surface scaffolds, as well as minimize the localized tissue response intrinsic to the current implanted device.

Declaration of Competing Interest

The authors declare that they have no known competing financial interests or personal relationships that could have appeared to influence the work reported in this paper.

Acknowledgments

We are thankful for financial support from the Brazilian Federal Agency for Support and Evaluation of Graduate Education (CAPES), State of São Paulo Research Foundation (FAPESP) (Thematic project # 2013/50181-1) and PRONON-SIPAR project #25000.077093/2015-86. I.R.C is thankful to Araucaria Foundation For Supporting Scientific and Technological Development of Paraná (058/2015). A.C.T is also thankful to FINEP (project # 01.10.0758.01) and CNPq-National Institute of Science and Technology-INCT of Nanobiotechnology (Project # 573880/2008-5) for the financial support.

Appendix A. Supplementary material

Supplementary data to this article can be found online at https://doi.org/10.1016/j.eurpolymj.2020.109621.

References

[1] J. Zhang, T.M. Woodruff, R.J. Clark, D.J. Martin, R.F. Minchin, Release of bioactive peptides from polyurethane films in vitro and in vivo: Effect of polymer composition, Acta Biomater. 41 (2016) 264–272.

[2] S. Ahn, C.O. Chantre, A.R. Gannon, J.U. Lind, P.H. Campbell, T. Grevesse, B.B. O'Connor, K.K. Parker, Soy protein/cellulose nanofiber scaffolds mimicking skin extracellular matrix for enhanced wound healing, Adv. Healthcare Mater. 7 (2018) 1701175.

[3] Y. Liu, X.Z. Shu, G.D. Prestwich, Osteochondral defect repair with autologous bone marrow–derived mesenchymal stem cells in an injectable, in situ, cross-linked synthetic extracellular matrix, Tissue Eng. 12 (2006) 3405–3416.

[4] R. Liu, X. Kuang, J. Deng, Y.C. Wang, A.C. Wang, W. Ding, Y.C. Lai, J. Chen, P. Wang, Z. Lin, Shape memory polymers for body motion energy harvesting and self-powered mechanosensing, Adv. Mater. 30 (2018) 1705195.

[5] N. Theodore, R. Hlubek, J. Danielson, K. Neff, L. Vaickus, T.R. Ulich, A.E. Ropper, First human implantation of a bioresorbable polymer scaffold for acute traumatic spinal cord injury: a clinical pilot study for safety and feasibility, Neurosurgery 79 (2016) E305–E312.

[6] H.-L. Kim, G.-Y. Jung, J.-H. Yoon, J.-S. Han, Y.-J. Park, D.-G. Kim, M. Zhang, D.-J. Kim, Preparation and characterization of nano-sized hydroxyapatite/alginate/chitosan composite scaffolds for bone tissue engineering, Mater. Sci. Eng., C 54 (2015) 20–25.

[7] Y. Zhang, J. Zhao, G. Yang, Y. Zhou, W. Gao, G. Wu, X. Li, C. Mao, T. Sheng, M. Zhou, Mechanical properties and degradation of drug eluted bioresorbable vascular scaffolds prepared by three-dimensional printing technology, J. Biomater. Sci. Polym. Ed. 30 (2019) 547–560.

[8] U. Sharma, D. Concagh, L. Core, Y. Kuang, C. You, Q. Pham, G. Zugates, R. Busold, S. Webber, J. Merlo, The development of bioresorbable composite polymeric implants with high mechanical strength, Nat. Mater. 17 (2018) 96.

[9] G. Tiwari, R. Tiwari, B. Sriwastawa, L. Bhati, S. Pandey, P. Pandey, S.K. Bannerjee, Drug delivery systems: an updated review, Int. J. Pharm. Invest. 2 (2012) 2.

[10] B. Baumann, T. Jungst, S. Stichler, S. Feineis, O. Wiltschka, M. Kuhlmann, M. Lindén, J. Groll, Control of nanoparticle release kinetics from 3D printed hydrogel scaffolds, Angew. Chem. Int. Ed. 56 (2017) 4623–4628.

[11] B. Ardeshirzadeh, N.A. Anaraki, M. Irani, L.R. Rad, S. Shamshiri, Controlled release of doxorubicin from electrospun PEO/chitosan/graphene oxide nanocomposite nanofibrous scaffolds, Mater. Sci. Eng., C 48 (2015) 384–390.

[12] S. Papa, I. Vismara, A. Mariani, M. Barilani, S. Rimondo, M. De Paola, N. Panini, E. Erba, E. Mauri, F. Rossi, Mesenchymal stem cells encapsulated into biomimetic hydrogel scaffold gradually release CCL2 chemokine in situ preserving cytoarchitecture and promoting functional recovery in spinal cord injury, J. Control. Release 278 (2018) 49–56.

[13] Y. Hu, J. Ran, Z. Zheng, Z. Jin, X. Chen, Z. Yin, C. Tang, Y. Chen, J. Huang, H. Le, Exogenous stromal derived factor-1 releasing silk scaffold combined with intra-articular injection of progenitor cells promotes bone-ligament-bone regeneration, Acta Biomater. 71 (2018) 168–183.

[14] W. Shi, M. Sun, X. Hu, B. Ren, J. Cheng, C. Li, X. Duan, X. Fu, J. Zhang, H. Chen, Structurally and functionally optimized silk-fibroin–gelatin scaffold using 3D printing to repair cartilage injury in vitro and in vivo, Adv. Mater. 29 (2017) 1701089.

[15] M. Ronga, A. Fagetti, G. Canton, E. Paiusco, M.F. Surace, P. Cherubino, Clinical applications of growth factors in bone injuries: experience with BMPs, Injury 44 (2013) S34–S39.

[16] S. Stegen, N. van Gastel, G. Carmeliet, Bringing new life to damaged bone: the importance of angiogenesis in bone repair and regeneration, Bone 70 (2015) 19–27.

[17] H. Cheng, W. Jiang, F.M. Phillips, R.C. Haydon, Y. Peng, L. Zhou, H.H. Luu, N. An, B. Breyer, P. Vanichakarn, Osteogenic activity of the fourteen types of human bone morphogenetic proteins (BMPs), JBJS 85 (2003) 1544–1552.

[18] S. Nagarajan, S. Radhakrishnan, S.N. Kalkura, S. Balme, P. Miele, M. Bechelany, Overview of protein-based biopolymers for biomedical application, Macromol. Chem. Phys. (2019) 1900126.

[19] Y. Wang, D.D. Rudym, A. Walsh, L. Abrahamsen, H.-J. Kim, H.S. Kim, C. Kirker-Head, D.L. Kaplan, In vivo degradation of three-dimensional silk fibroin scaffolds, Biomaterials 29 (2008) 3415–3428.

[20] B.D. Ratner, A.S. Hoffman, F.J. Schoen, J.E. Lemons, Biomaterials Science: An Introduction to Materials in Medicine, Elsevier, 2004.

[21] M. Tsukada, G. Freddi, Y. Gotoh, N. Kasai, Physical and chemical properties of tussah silk fibroin films, J. Polym. Sci., Part B: Polym. Phys. 32 (1994) 1407–1412.

[22] A.R. Murphy, D.L. Kaplan, Biomedical applications of chemically-modified silk fibroin, J. Mater. Chem. 19 (2009) 6443–6450.

[23] T. Asakura, Y. Watanabe, A. Uchida, H. Minagawa, NMR of silk fibroin. Carbon-13 NMR study of the chain dynamics and solution structure of Bombyx mori silk fibroin, Macromolecules 17 (1984) 1075–1081.

[24] G.L. Ackland, A.G. Del Arroyo, S.T. Yao, R.C. Stephens, A. Dyson, N.J. Klein, M. Singer, A.V. Gourine, Low-molecular-weight polyethylene glycol improves survival in experimental sepsis, Crit. Care Med. 38 (2010) 629–636.

[25] R. Fernandez-Serra, R. Gallego, P. Lozano, D. González-Nieto, Hydrogels for neuroprotection and functional rewiring: a new era for brain engineering, Neural Regener. Res. 15 (2020) 783.

[26] Y. Martín-Martín, L. Fernández-García, M.H. Sanchez-Rebato, N. Marí-Buyé, F.J. Rojo, J. Pérez-Rigueiro, M. Ramos, G.V. Guinea, F. Panetsos, D. González-Nieto, Evaluation of neurosecretome from mesenchymal stem cells encapsulated in silk fibroin hydrogels, Sci. Rep. 9 (2019) 8801.

[27] D. Sood, M. Tang-Schomer, D. Pouli, C. Mizzoni, N. Raia, A. Tai, K. Arkun, J. Wu, L.D. Black, B. Scheffler, 3D extracellular matrix microenvironment in bioengineered tissue models of primary pediatric and adult brain tumors, Nat. Commun. 10 (2019) 1–14.

[28] Y. Chen, T. Wu, S. Huang, C.-W.W. Suen, X. Cheng, J. Li, H. Hou, G. She, H. Zhang, H. Wang, Sustained release SDF-1α/TGF-β1-loaded silk fibroin-porous gelatin scaffold promotes cartilage repair, ACS Appl. Mater. Interfaces 11 (2019) 14608–14618.

[29] B. Yavuz, J.L. Morgan, C. Herrera, K. Harrington, B. Perez-Ramirez, P.J. LiWang, D.L. Kaplan, Sustained release silk fibroin discs: antibody and protein delivery for HIV prevention, J. Control. Release 301 (2019) 1–12.

[30] J.E.U. Rojas, B.B. Gerbelli, A.O. Ribeiro, I.L. Nantes-Cardoso, F. Giuntini, W.A. Alves, Silk fibroin hydrogels for potential applications in photodynamic therapy, Biopolymers 110 (2019) e23245.

[31] M.J. Buehler, Nature designs tough collagen: explaining the nanostructure of collagen fibrils, Proc. Natl. Acad. Sci. 103 (2006) 12285–12290.

[32] K. Silvipriya, K.K. Kumar, A. Bhat, B.D. Kumar, A. John, P. Lakshmanan, Collagen: animal sources and biomedical application, J. Appl. Pharm. Sci. 5 (2015) 123–127.

[33] R.M. Raftery, D.P. Walsh, L.B. Ferreras, I.M. Castaño, G. Chen, M. LeMoine, G. Osman, K.M. Shakesheff, J.E. Dixon, F.J. O'Brien, Highly versatile cell-penetrating peptide loaded scaffold for efficient and localized gene delivery to multiple cell types: from development to application in tissue engineering, Biomaterials (2019) 119277.

[34] F. Dosio, S. Arpicco, B. Stella, E. Fattal, Hyaluronic acid for anticancer drug and nucleic acid delivery, Adv. Drug Deliv. Rev. 97 (2016) 204–236.

[35] D. Zhu, H. Wang, P. Trinh, S.C. Heilshorn, F. Yang, Elastin-like protein-hyaluronic acid (ELP-HA) hydrogels with decoupled mechanical and biochemical cues for cartilage regeneration, Biomaterials 127 (2017) 132–140.

[36] J. Zhu, F. Li, X. Wang, J. Yu, D. Wu, Hyaluronic acid and polyethylene glycol hybrid hydrogel encapsulating nanogel with hemostasis and sustainable antibacterial property for wound healing, ACS Appl. Mater. Interfaces 10 (2018) 13304–13316.

[37] S. Emoto, H. Yamaguchi, T. Kamei, H. Ishigami, T. Suhara, Y. Suzuki, T. Ito, J. Kitayama, T. Watanabe, Intraperitoneal administration of cisplatin via an in situ cross-linkable hyaluronic acid-based hydrogel for peritoneal dissemination of gastric cancer, Surg. Today 44 (2014) 919–926.

[38] M. Rezazadeh, V. Akbari, E. Amuaghae, J. Emami, Preparation and characterization of an injectable thermosensitive hydrogel for simultaneous delivery of paclitaxel and doxorubicin, Res. Pharm. Sci. 13 (2018) 181.

[39] G. Bajaj, M.R. Kim, S.I. Mohammed, Y. Yeo, Hyaluronic acid-based hydrogel for regional delivery of paclitaxel to intraperitoneal tumors, J. Control. Release 158 (2012) 386–392.

[40] L.A. Gurski, A.K. Jha, C. Zhang, X. Jia, M.C. Farach-Carson, Hyaluronic acid-based hydrogels as 3D matrices for in vitro evaluation of chemotherapeutic drugs using poorly adherent prostate cancer cells, Biomaterials 30 (30) (2009) 6076–6085.

[41] K. Xu, F. Lee, S.J. Gao, J.E. Chung, H. Yano, M. Kurisawa, Injectable hyaluronic acid-tyramine hydrogels incorporating interferon-α2a for liver cancer therapy, J. Control. Release 166 (2013) 203–210.

[42] P. Gibbs, P.R. Clingan, V. Ganju, A.H. Strickland, S.S. Wong, N.C. Tebbutt, C.R. Underhill, R.M. Fox, S.P. Clavant, J. Leung, Hyaluronan-Irinotecan improves progression-free survival in 5-fluorouracil refractory patients with metastatic colorectal cancer: a randomized phase II trial, Cancer Chemother. Pharmacol. 67 (2011) 153–163.

[43] J. Venkatesan, I. Bhatnagar, P. Manivasagan, K.-H. Kang, S.-K. Kim, Alginate composites for bone tissue engineering: a review, Int. J. Biol. Macromol. 72 (2015) 269–281.

[44] S.R. Moxon, N.J. Corbett, K. Fisher, G. Potjewyd, M. Domingos, N.M. Hooper, Blended alginate/collagen hydrogels promote neurogenesis and neuronal maturation, Mater. Sci. Eng., C (2019) 109904.

[45] Q.Z. Wang, X.G. Chen, N. Liu, S.X. Wang, C.S. Liu, X.H. Meng, C.G. Liu, Protonation constants of chitosan with different molecular weight and degree of deacetylation, Carbohydr. Polym. 65 (2006) 194–201.

[46] C. Qin, H. Li, Q. Xiao, Y. Liu, J. Zhu, Y. Du, Water-solubility of chitosan and its antimicrobial activity, Carbohydr. Polym. 63 (2006) 367–374.

[47] K. Kalantari, A.M. Afifi, H. Jahangirian, T.J. Webster, Biomedical applications of chitosan electrospun nanofibers as a green polymer–review, Carbohydr. Polym. (2018).

[48] I. Bano, M. Arshad, T. Yasin, M.A. Ghauri, Preparation, characterization and evaluation of glycerol plasticized chitosan/PVA blends for burn wounds, Int. J. Biol. Macromol. 124 (2019) 155–162.

[49] S. Fakirov, Z. Sarac, T. Anbar, B. Boz, I. Bahar, M. Evstatiev, A. Apostolov, J. Mark, A. Kloczkowski, Mechanical properties and transition temperatures of crosslinked-oriented gelatin, Colloid Polym. Sci. 275 (1997) 307–314.

[50] J.M. Dang, K.W. Leong, Natural polymers for gene delivery and tissue engineering, Adv. Drug Deliv. Rev. 58 (2006) 487–499.

[51] W.H. Binder, The past 40 years of macromolecular sciences: reflections on challenges in synthetic polymer and material science, Macromol. Rapid Commun. 40 (2019) 1800610.

[52] S.J. Cho, S.M. Jung, M. Kang, H.S. Shin, J.H. Youk, Preparation of hydrophilic PCL nanofiber scaffolds via electrospinning of PCL/PVP-b-PCL block copolymers for enhanced cell biocompatibility, Polymer 69 (2015) 95–102.

[53] X. Farto-Vaamonde, G. Auriemma, R.P. Aquino, A. Concheiro, C. Alvarez-Lorenzo, Post-manufacture loading of filaments and 3D printed PLA scaffolds with prednisolone and dexamethasone for tissue regeneration applications, Eur. J. Pharm. Biopharm. 141 (2019) 100–110.

[54] Y. Zhang, J. Wang, J. Xiao, T. Fang, N. Hu, M. Li, L. Deng, Y. Cheng, Y. Zhu, W. Cui, An electrospun fiber-covered stent with programmable dual drug release for endothelialization acceleration and lumen stenosis prevention, Acta Biomater. (2019).

[55] E. Llorens, S. Calderón, L.J. del Valle, J. Puiggalí, Polybiguanide (PHMB) loaded in PLA scaffolds displaying high hydrophobic, biocompatibility and antibacterial

properties, Mater. Sci. Eng., C 50 (2015) 74–84.
[56] J. Dai, J. Jin, S. Yang, G. Li, Doxorubicin-loaded PLA/pearl electrospun nanofibrous scaffold for drug delivery and tumor cell treatment, Mater. Res. Express 4 (2017) 075403.
[57] H. Yin, G. Ding, X. Shi, W. Guo, Z. Ni, H. Fu, Z. Fu, A bioengineered drug-Eluting scaffold accelerated cutaneous wound healing In diabetic mice, Colloids Surf. B: Biointerfaces 145 (2016) 226–231.
[58] Y. Liu, T. Nelson, B. Cromeens, T. Rager, J. Lannutti, J. Johnson, G.E. Besner, HB-EGF embedded in PGA/PLLA scaffolds via subcritical CO2 augments the production of tissue engineered intestine, Biomaterials 103 (2016) 150–159.
[59] R. García-Alvarez, I. Izquierdo-Barba, M. Vallet-Regí, 3D scaffold with effective multidrug sequential release against bacteria biofilm, Acta Biomater. 49 (2017) 113–126.
[60] X.-H. Zhou, D.-X. Wei, H.-M. Ye, X. Zhang, X. Meng, Q. Zhou, Development of poly (vinyl alcohol) porous scaffold with high strength and well ciprofloxacin release efficiency, Mater. Sci. Eng., C 67 (2016) 326–335.
[61] T.N. da Silva, R.P. Gonçalves, C.L. Rocha, B.S. Archanjo, C.A.G. Barboza, M.B.R. Pierre, F. Reynaud, P.H. de Souza Picciani, Controlling burst effect with PLA/PVA coaxial electrospun scaffolds loaded with BMP-2 for bone guided regeneration, Mater. Sci. Eng.: C 97 (2019) 602–612.
[62] E. Yilgör, M. Isik, C.K. Söz, I. Yilgör, Synthesis and structure-property behavior of polycaprolactone-polydimethylsiloxane-polycaprolactone triblock copolymers, Polymer 83 (2016) 138–153.
[63] K. Shi, Y.-L. Wang, Y. Qu, J.-F. Liao, B.-Y. Chu, H.-P. Zhang, F. Luo, Z.-Y. Qian, Synthesis, characterization, and application of reversible PDLLA-PEG-PDLLA copolymer thermogels in vitro and in vivo, Sci. Rep. 6 (2016) 19077.
[64] R.A. Dilla, C.M. Motta, S.R. Snyder, J.A. Wilson, C. Wesdemiotis, M.L. Becker, Synthesis and 3D printing of PEG–poly (propylene fumarate) diblock and triblock copolymer hydrogels, ACS Macro Lett. 7 (2018) 1254–1260.
[65] W. Wu, Triblock copolymers of PLLA-PEG-PLLA for nerve guidance channel scaffolds via 3D printing, Northeastern University, 2017.
[66] A. Abbadessa, V.H. Mouser, M.M. Blokzijl, D. Gawlitta, W.J. Dhert, W.E. Hennink, J. Malda, T. Vermonden, A synthetic thermosensitive hydrogel for cartilage bioprinting and its biofunctionalization with polysaccharides, Biomacromolecules 17 (2016) 2137–2147.
[67] R. Perret, A. Skoulios, Synthèse et caractérisation de copolymères séquencés polyoxyéthylène/poly-ε-caprolactone, Die Makromolekulare Chemie: Macromolecular Chemistry and Physics 156 (1) (1972) 143–156.
[68] H. Deng, A. Dong, J. Song, X. Chen, Injectable thermosensitive hydrogel systems based on functional PEG/PCL block polymer for local drug delivery, J. Control. Release 297 (2019) 60–70.
[69] G.-W. Jeong, W.-G. Hong, J.-H. Anh, Y.-J. Jeon, S.S. Choi, T.-I. Son, S.C. Kim, Y.-I. Jeong, J.-W. Nah, Anticancer effect of intracellular-delivered paclitaxel using novel pH-sensitive LMWSC-PCL di-block copolymer micelles, J. Indust. Eng. Chem. 70 (2019) 136–144.
[70] L. Song, M.F. Ahmed, Y. Li, J. Bejoy, C. Zeng, Y. Li, PCL-PDMS-PCL copolymer-based microspheres mediate cardiovascular differentiation from embryonic stem cells, Tissue Eng. Part C: Methods 23 (2017) 627–640.
[71] T. Öztürk, K.A. Cavicchi, Synthesis and characterization of poly (epichlorohydrin-g-ε-caprolactone) graft copolymers by“ click” chemistry, J. Polym. Mater. 35 (2) (2018) 209–220.
[72] D. Han, T.-J. Wen, G. Han, Y.-Y. Deng, Y. Deng, Q. Zhang, Q. Fu, Synthesis of Janus POSS star polymer and exploring its compatibilization behavior for PLLA/PCL polymer blends, Polymer 136 (2018) 84–91.
[73] F. Oroojalian, Z. Jahanafrooz, F. Chogan, A.H. Rezayan, E. Malekzade, S.J.T. Rezaei, M.R. Nabid, A. Sahebkar, Synthesis and evaluation of injectable thermosensitive penta-block copolymer hydrogel (PNIPAAm-PCL-PEG-PCL-PNIPAAm) and star-shaped poly (CL— CO— LA)-b-PEG for wound healing applications, J. Cell. Biochem. (2019).
[74] S. Saghebasl, S. Davaran, R. Rahbarghazi, A. Montaseri, R. Salehi, A. Ramazani, Synthesis and in vitro evaluation of thermosensitive hydrogel scaffolds based on (PNIPAAm-PCL-PEG-PCL-PNIPAAm)/Gelatin and (PCL-PEG-PCL)/Gelatin for use in cartilage tissue engineering, J. Biomater. Sci. Polym. Ed. 29 (2018) 1185–1206.
[75] H. Qiu, Z. Yang, M.I. Shah, Z. Mao, J. Ling, [PCL-bP (THF-co-CL)] m multiblock copolymer synthesized by Janus polymerization, Polymer 128 (2017) 71–77.
[76] Y.Y. Yuan, C.Q. Mao, X.J. Du, J.Z. Du, F. Wang, J. Wang, Surface charge switchable nanoparticles based on zwitterionic polymer for enhanced drug delivery to tumor, Adv. Mater. 24 (40) (2012) 5476–5480.
[77] C.-F. Huang, W.-H. Chen, J. Aimi, Y.-S. Huang, S. Venkatesan, Y.-W. Chiang, S.-H. Huang, S.-W. Kuo, T. Chen, Synthesis of well-defined PCL-b-PnBA-b-PMMA ABC-type triblock copolymers: toward the construction of nanostructures in epoxy thermosets, Polym. Chem. 9 (2018) 5644–5654.
[78] G.Z. Yin, X.M. Yang, Q.F. Li, Influences of terminal POSS on crystallization and degradation behavior of PCL-PLLA block copolymer, Polym. Crystall. 1 (2018) e10019.
[79] H. Nosrati, P. Barzegari, H. Danafar, H. Kheiri Manjili, Biotin-functionalized copolymeric PEG-PCL micelles for in vivo tumour-targeted delivery of artemisinin, Artificial Cells, Nanomed., Biotechnol. 47 (2019) 104–114.
[80] S. Petrova, D. Klepac, R. Konefał, S. Kereïche, L.R. Kováčik, S.K. Filippov, Synthesis and solution properties of PCL-b-PHPMA diblock copolymers containing stable nitroxyl radicals, Macromolecules 49 (2016) 5407–5417.
[81] L. Zou, A.S. Braegelman, M.J. Webber, Dynamic supramolecular hydrogels spanning an unprecedented range of host-guest affinity, ACS Appl. Mater. Interfaces (2019).
[82] A. Metters, J. Hubbell, Network formation and degradation behavior of hydrogels formed by Michael-type addition reactions, Biomacromolecules 6 (2005) 290–301.
[83] E.M. Anderson, M.L. Noble, S. Garty, H. Ma, J.D. Bryers, T.T. Shen, B.D. Ratner, Sustained release of antibiotic from poly (2-hydroxyethyl methacrylate) to prevent blinding infections after cataract surgery, Biomaterials 30 (2009) 5675–5681.
[84] T.L. Sun, T. Kurokawa, S. Kuroda, A.B. Ihsan, T. Akasaki, K. Sato, M.A. Haque, T. Nakajima, J.P. Gong, Physical hydrogels composed of polyampholytes demonstrate high toughness and viscoelasticity, Nat. Mater. 12 (2013) 932.
[85] J. Li, E. Weber, S. Guth-Gundel, M. Schuleit, A. Kuttler, C. Halleux, N. Accart, A. Doelemeyer, A. Basler, B. Tigani, Tough composite hydrogels with high loading and local release of biological drugs, Adv. Healthcare Mater. 7 (2018).
[86] H.-W. Kang, S.J. Lee, I.K. Ko, C. Kengla, J.J. Yoo, A. Atala, A 3D bioprinting system to produce human-scale tissue constructs with structural integrity, Nat. Biotechnol. 34 (2016) 312.
[87] B. Dorj, J.-E. Won, O. Purevdorj, K.D. Patel, J.-H. Kim, E.-J. Lee, H.-W. Kim, A novel therapeutic design of microporous-structured biopolymer scaffolds for drug loading and delivery, Acta Biomater. 10 (2014) 1238–1250.
[88] T. Weigel, G. Schinkel, A. Lendlein, Design and preparation of polymeric scaffolds for tissue engineering, Expert Rev. Med. Devices 3 (2006) 835–851.
[89] S. Ramakrishna, An Introduction to Electrospinning and Nanofibers, World Scientific, 2005.
[90] J.F. Cooley, Apparatus for electrically dispersing fluids, Google Patents, 1902.
[91] W.J. Morton, Method of dispersing fluids, Google Patents, 1902.
[92] A. Gora, R. Sahay, V. Thavasi, S. Ramakrishna, Melt-electrospun fibers for advances in biomedical engineering, clean energy, filtration, and separation, Polym. Rev. 51 (2011) 265–287.
[93] T.D. Brown, P.D. Dalton, D.W. Hutmacher, Melt electrospinning today: an opportune time for an emerging polymer process, Prog. Polym. Sci. 56 (2016) 116–166.
[94] H. Lian, Z. Meng, Melt electrospinning vs. solution electrospinning: a comparative study of drug-loaded poly (ε-caprolactone) fibres, Mater. Sci. Eng.: C 74 (2017) 117–123.
[95] R. Sedghi, A. Shaabani, Electrospun biocompatible core/shell polymer-free core structure nanofibers with superior antimicrobial potency against multi drug resistance organisms, Polymer 101 (2016) 151–157.
[96] A. Haider, S. Haider, I.-K. Kang, A comprehensive review summarizing the effect of electrospinning parameters and potential applications of nanofibers in biomedical and biotechnology, Arabian J. Chem. 11 (2018) 1165–1188.
[97] A. Greiner, J.H. Wendorff, Electrospinning: a fascinating method for the preparation of ultrathin fibers, Angew. Chem. Int. Ed. 46 (2007) 5670–5703.
[98] X. Guo, J. Zhu, H. Zhang, Z. You, Y. Morsi, X. Mo, T. Zhu, Facile preparation of a controlled-release tubular scaffold for blood vessel implantation, J. Colloid Interface Sci. 539 (2019) 351–360.
[99] S. Chen, H. Wang, A. McCarthy, Z. Yan, H.J. Kim, M.A. Carlson, Y. Xia, J. Xie, Three-dimensional objects consisting of hierarchically assembled nanofibers with controlled alignments for regenerative medicine, Nano Lett. (2019).
[100] B. Jian, W. Wu, Y. Song, N. Tan, C. Ma, Microporous elastomeric membranes fabricated with polyglycerol sebacate improved guided bone regeneration in a rabbit model, Int. J. Nanomed. 14 (2019) 2683.
[101] B. Joseph, R. Augustine, N. Kalarikkal, S. Thomas, B. Seantier, Y. Grohens, Recent advances in electrospun polycaprolactone based scaffolds for wound healing and skin bioengineering applications, Mater. Today Commun. 19 (2019) 319–335.
[102] B.J. Kim, H. Cheong, E.S. Choi, S.H. Yun, B.H. Choi, K.S. Park, I.S. Kim, D.H. Park, H.J. Cha, A ccelerated skin wound healing using electrospun nanofibrous mats blended with mussel adhesive protein and polycaprolactone, J. Biomed. Mater. Res. Part A 105 (2017) 218–225.
[103] G. Tejada, G. Piccirilli, M. Sortino, C. Salomón, M. Lamas, D. Leonardi, Formulation and in-vitro efficacy of antifungal mucoadhesive polymeric matrices for the delivery of miconazole nitrate, Mater. Sci. Eng., C 79 (2017) 140–150.
[104] Y. Byun, S. Whiteside, R. Thomas, M. Dharman, J. Hughes, Y.T. Kim, The effect of solvent mixture on the properties of solvent cast polylactic acid (PLA) film, J. Appl. Polym. Sci. 124 (2012) 3577–3582.
[105] M. Lee, J.K. Park, H.-S. Lee, O. Lane, R.B. Moore, J.E. McGrath, D.G. Baird, Effects of block length and solution-casting conditions on the final morphology and properties of disulfonated poly (arylene ether sulfone) multiblock copolymer films for proton exchange membranes, Polymer 50 (2009) 6129–6138.
[106] P. Anbukarasu, D. Sauvageau, A. Elias, Tuning the properties of polyhydroxybutyrate films using acetic acid via solvent casting, Sci. Rep. 5 (2015) 17884.
[107] J. Becerra, G. Sudre, I. Royaud, R. Montserret, B. Verrier, C. Rochas, T. Delair, L. David, Tuning the hydrophilic/hydrophobic balance to control the structure of chitosan films and their protein release behavior, AAPS PharmSciTech 18 (2017) 1070–1083.
[108] R.S. Bhattarai, A. Das, R.M. Alzhrani, D. Kang, S.B. Bhaduri, S.H. Boddu, Comparison of electrospun and solvent cast polylactic acid (PLA)/poly (vinyl alcohol)(PVA) inserts as potential ocular drug delivery vehicles, Mater. Sci. Eng., C 77 (2017) 895–903.
[109] K. Ghosal, A. Chandra, G. Praveen, S. Snigdha, S. Roy, C. Agatemor, S. Thomas, I. Provaznik, Electrospinning over solvent casting: tuning of mechanical properties of membranes, Sci. Rep. 8 (2018) 5058.
[110] H.J. Park, O.J. Lee, M.C. Lee, B.M. Moon, H.W. Ju, J.M. Lee, J.-H. Kim, D.W. Kim, C.H. Park, Fabrication of 3D porous silk scaffolds by particulate (salt/sucrose) leaching for bone tissue reconstruction, Int. J. Biol. Macromol. 78 (2015) 215–223.
[111] S. Sayyar, D.L. Officer, G.G. Wallace, Fabrication of 3D structures from graphene-based biocomposites, J. Mater. Chem. B 5 (2017) 3462–3482.
[112] G.-W. Oetjen, P. Haseley, Freeze-Drying, John Wiley & Sons, 2004.
[113] A. Ogienko, V. Drebushchak, E. Bogdanova, A. Yunoshev, A. Ogienko,

E. Boldyreva, A.Y. Manakov, Thermodynamic aspects of freeze-drying, J. Therm. Anal. Calorim. 127 (2017) 1593–1604.
[114] C.W. Hull, Apparatus for production of three-dimensional objects by stereolithography, US Patent 4,575,330, 1986.
[115] L. Moroni, T. Boland, J.A. Burdick, C. De Maria, B. Derby, G. Forgacs, J. Groll, Q. Li, J. Malda, V.A. Mironov, Biofabrication: a guide to technology and terminology, Trends Biotechnol. 36 (2018) 384–402.
[116] N.A. Peppas, A.R. Khare, Preparation, structure and diffusional behavior of hydrogels in controlled release, Adv. Drug Deliv. Rev. 11 (1993) 1–35.
[117] B. Vázquez, J. San Roman, C. Peniche, M.E. Cohen, Polymeric hydrophilic hydrogels with flexible hydrophobic chains. Control of the hydration and interactions with water molecules, Macromolecules 30 (1997) 8440–8446.
[118] L. Vinet, A. Zhedanov, A 'missing'family of classical orthogonal polynomials, J. Phys. A: Math. Theor. 44 (2011) 085201.
[119] R. Bossoni, A. Riul, A.J. Valente, A.F. Rubira, E.C. Muniz, Release of vitamin B12 and diclofenac potassium from N, N-dimethylacrylamide-modified arabic gum hydrogels-the partition-diffusion model, J. Braz. Chem. Soc. 25 (2014) 1124–1134.
[120] F. Alhaique, M.A. Casadei, C. Cencetti, T. Coviello, C. Di Meo, P. Matricardi, E. Montanari, S. Pacelli, P. Paolicelli, From macro to nano polysaccharide hydrogels: an opportunity for the delivery of drugs, J. Drug Delivery Sci. Technol. 32 (2016) 88–99.
[121] F. Ullah, M.B.H. Othman, F. Javed, Z. Ahmad, H.M. Akil, Classification, processing and application of hydrogels: a review, Mater. Sci. Eng.: C 57 (2015) 414–433.
[122] W.E. Hennink, C.F. van Nostrum, Novel crosslinking methods to design hydrogels, Adv. Drug Deliv. Rev. 64 (2012) 223–236.
[123] S.A. Poursamar, A.N. Lehner, M. Azami, S. Ebrahimi-Barough, A. Samadikuchaksaraei, A.P.M. Antunes, The effects of crosslinkers on physical, mechanical, and cytotoxic properties of gelatin sponge prepared via in-situ gas foaming method as a tissue engineering scaffold, Mater. Sci. Eng., C 63 (2016) 1–9.
[124] R.Y. Tam, J. Yockell-Lelièvre, L.J. Smith, L.M. Julian, A.E. Baker, C. Choey, M.S. Hasim, J. Dimitroulakos, W.L. Stanford, M.S. Shoichet, Rationally designed 3D hydrogels model invasive lung diseases enabling high-content drug screening, Adv. Mater. 31 (2019) 1806214.
[125] W. Hu, Z. Wang, Y. Xiao, S. Zhang, J. Wang, Advances in crosslinking strategies of biomedical hydrogels, Biomater. Sci. 7 (2019) 843–855.
[126] F.J. Vernerey, E.C. Greenwald, S.J. Bryant, Triphasic mixture model of cell-mediated enzymatic degradation of hydrogels, Comput. Methods Biomech. Biomed. Eng. 15 (2012) 1197–1210.
[127] A.P. Gerola, D.C. Silva, A.F. Matsushita, O. Borges, A.F. Rubira, E.C. Muniz, A.J. Valente, The effect of methacrylation on the behavior of Gum Arabic as pH-responsive matrix for colon-specific drug delivery, Eur. Polym. J. 78 (2016) 326–339.
[128] E. Andrzejewska, Free-radical photopolymerization of multifunctional monomers, Three-Dimensional Microfabrication Using Two-Photon Polymerization, Elsevier, 2020, pp. 77–99.
[129] Y. Wang, Z. Liu, C. Zhou, Y. Yuan, L. Jiang, B. Wu, J. Lei, A facile strategy for high performance recyclable polymer systems via dynamic metal ion crosslinking, J. Mater. Chem. A 7 (2019) 3577–3582.
[130] K. Joyner, D. Song, R.F. Hawkins, R.D. Silcott, G.A. Duncan, A rational approach to form disulfide linked mucin hydrogels, Soft Matter 15 (2019) 9632–9639.
[131] S.A. Elkassih, P. Kos, H. Xiong, D.J. Siegwart, Degradable redox-responsive disulfide-based nanogel drug carriers via dithiol oxidation polymerization, Biomater. Sci. 7 (2019) 607–617.
[132] H. Arimoto, M. Egawa, Imaging wavelength and light penetration depth for water content distribution measurement of skin, Skin Res. Technol. 21 (2015) 94–100.
[133] S. Ahmad, M. Ahmad, K. Manzoor, R. Purwar, S. Ikram, A review on latest innovations in natural gums based hydrogels: preparations & applications, Int. J. Biol. Macromol. (2019).
[134] S. Chatterjee, P.C.-l. Hui, C.-W. Kan, W. Wang, Dual-responsive (pH/temperature) Pluronic F-127 hydrogel drug delivery system for textile-based transdermal therapy, Sci. Reports 9 (2019) 1–13.
[135] P. Worthington, S. Langhans, D. Pochan, β-Hairpin peptide hydrogels for package delivery, Adv. Drug Deliv. Rev. 110 (2017) 127–136.
[136] J. Liu, C.S.Y. Tan, Y. Lan, O.A. Scherman, Aqueous polymer self-assembly based on cucurbit [n] uril-mediated host-guest interactions, Macromol. Chem. Phys. 217 (2016) 319–332.
[137] M. Ni, N. Zhang, W. Xia, X. Wu, C. Yao, X. Liu, X.-Y. Hu, C. Lin, L. Wang, Dramatically promoted swelling of a hydrogel by pillar [6] arene–ferrocene complexation with multistimuli responsiveness, J. Am. Chem. Soc. 138 (2016) 6643–6649.
[138] H. Yang, J. Tang, C. Shang, R. Miao, S. Zhang, K. Liu, Y. Fang, Calix [4] arene-based dynamic covalent gels: marriage of robustness, responsiveness, and self-healing, Macromol. Rapid Commun. 39 (2018) 1700679.
[139] C.B. Rodell, M.E. Lee, H. Wang, S. Takebayashi, T. Takayama, T. Kawamura, J.S. Arkles, N.N. Dusaj, S.M. Dorsey, W.R. Witschey, Injectable shear-thinning hydrogels for minimally invasive delivery to infarcted myocardium to limit left ventricular remodeling, Circulation: Cardiovasc. Intervent. 9 (2016).
[140] C.B. Rodell, J.W. MacArthur Jr, S.M. Dorsey, R.J. Wade, L.L. Wang, Y.J. Woo, J.A. Burdick, Shear-thinning supramolecular hydrogels with secondary autonomous covalent crosslinking to modulate viscoelastic properties in vivo, Adv. Funct. Mater. 25 (2015) 636–644.
[141] R.C. Gorman, B.M. Jackson, J.A. Burdick, J.H. Gorman, Infarct restraint to limit adverse ventricular remodeling, J. Cardiovasc. Translat. Res. 4 (2011) 73–81.
[142] M.M. Bastings, S. Koudstaal, R.E. Kieltyka, Y. Nakano, A. Pape, D.A. Feyen, F.J. Van Slochteren, P.A. Doevendans, J.P. Sluijter, E. Meijer, A fast pH-switchable and self-healing supramolecular hydrogel carrier for guided, local catheter injection in the infarcted myocardium, Adv. Healthcare Mater. 3 (2014) 70–78.
[143] A.V. Boopathy, M.D. Martinez, A.W. Smith, M.E. Brown, A.J. García, M.E. Davis, Intramyocardial delivery of notch ligand-containing hydrogels improves cardiac function and angiogenesis following infarction, Tissue Eng. Part A 21 (2015) 2315–2322.
[144] H. Zhu, X. Li, M. Yuan, W. Wan, M. Hu, X. Wang, X. Jiang, Intramyocardial delivery of bFGF with a biodegradable and thermosensitive hydrogel improves angiogenesis and cardio-protection in infarcted myocardium, Exp. Therap. Med. 14 (2017) 3609–3615.
[145] H. Zhu, X. Jiang, X. Li, M. Hu, W. Wan, Y. Wen, Y. He, X. Zheng, Intramyocardial delivery of VEGF 165 via a novel biodegradable hydrogel induces angiogenesis and improves cardiac function after rat myocardial infarction, Heart Vessels 31 (2016) 963–975.
[146] L.L. Wang, Y. Liu, J.J. Chung, T. Wang, A.C. Gaffey, M. Lu, C.A. Cavanaugh, S. Zhou, R. Kanade, P. Atluri, Sustained miRNA delivery from an injectable hydrogel promotes cardiomyocyte proliferation and functional regeneration after ischaemic injury, Nat. Biomed. Eng. 1 (2017) 983.
[147] Y. Chen, J. Shi, Y. Zhang, J. Miao, Z. Zhao, X. Jin, L. Liu, L. Yu, C. Shen, J. Ding, An injectable thermosensitive hydrogel loaded with an ancient natural drug colchicine for myocardial repair after infarction, J. Mater. Chem. B (2020).
[148] D.E. Soranno, C.B. Rodell, C. Altmann, J. Duplantis, A. Andres-Hernando, J.A. Burdick, S. Faubel, Delivery of interleukin-10 via injectable hydrogels improves renal outcomes and reduces systemic inflammation following ischemic acute kidney injury in mice, Am. J. Physiol.-Renal Physiol. 311 (2016) F362–F372.
[149] Y. Zhang, L. Tao, S. Li, Y. Wei, Synthesis of multiresponsive and dynamic chitosan-based hydrogels for controlled release of bioactive molecules, Biomacromolecules 12 (2011) 2894–2901.
[150] L. Yang, Y. Li, Y. Gou, X. Wang, X. Zhao, L. Tao, Improving tumor chemotherapy effect using an injectable self-healing hydrogel as drug carrier, Polym. Chem. 8 (2017) 5071–5076.
[151] X. Zhou, Y. Li, S. Chen, Y.-N. Fu, S. Wang, G. Li, L. Tao, Y. Wei, X. Wang, J.F. Liang, Dynamic agent of an injectable and self-healing drug-loaded hydrogel for embolization therapy, Colloids Surf., B 172 (2018) 601–607.
[152] Y. Li, Y. Zhang, F. Shi, L. Tao, Y. Wei, X. Wang, Modulus-regulated 3D-cell proliferation in an injectable self-healing hydrogel, Colloids Surf., B 149 (2017) 168–173.
[153] Z.L. Pianowski, J. Karcher, K. Schneider, Photoresponsive self-healing supramolecular hydrogels for light-induced release of DNA and doxorubicin, Chem. Commun. 52 (2016) 3143–3146.
[154] L. Shi, Y. Han, J. Hilborn, D. Ossipov, "Smart" drug loaded nanoparticle delivery from a self-healing hydrogel enabled by dynamic magnesium–biopolymer chemistry, Chem. Commun. 52 (2016) 11151–11154.
[155] J. Chen, S. Li, Y. Zhang, W. Wang, X. Zhang, Y. Zhao, Y. Wang, H. Bi, A reloadable self-healing hydrogel enabling diffusive transport of C-dots across gel-gel interface for scavenging reactive oxygen species, Adv. Healthcare Mater. 6 (2017) 1700746.
[156] F. Meng, V. Dave, H. Chauhan, Qualitative and quantitative methods to determine miscibility in amorphous drug–polymer systems, Eur. J. Pharm. Sci. 77 (2015) 106–111.
[157] S. Seif, L. Franzen, M. Windbergs, Overcoming drug crystallization in electrospun fibers–elucidating key parameters and developing strategies for drug delivery, Int. J. Pharm. 478 (2015) 390–397.
[158] G. Houen, K. Bechgaard, K. Bechgaard, J. Songstad, M. Leskelä, M. Polamo, The solubility of proteins in organic solvents, Acta Chem. Scand. 50 (1996) 68–70.
[159] S. Hengsawas Surasarang, J.M. Keen, S. Huang, F. Zhang, J.W. McGinity, R.O. Williams III, Hot melt extrusion versus spray drying: hot melt extrusion degrades albendazole, Drug Dev. Ind. Pharm. 43 (2017) 797–811.
[160] C.-C. Lin, A.T. Metters, Hydrogels in controlled release formulations: network design and mathematical modeling, Adv. Drug Deliv. Rev. 58 (2006) 1379–1408.
[161] G.D. Prestwich, Hyaluronic acid-based clinical biomaterials derived for cell and molecule delivery in regenerative medicine, J. Control. Release 155 (2011) 193–199.
[162] L. Cao, Y. Yu, J. Wang, J.A. Werkmeister, K.M. McLean, C. Liu, 2-N, 6-O-sulfated chitosan-assisted BMP-2 immobilization of PCL scaffolds for enhanced osteoinduction, 74 (2017) 298–306.
[163] S.K. Nemani, R.K. Annavarapu, B. Mohammadian, A. Raiyan, J. Heil, M.A. Haque, A. Abdelaal, H. Sojoudi, Surface modification of polymers: methods and applications, Adv. Mater. Interfaces 5 (2018) 1801247.
[164] J.-R. Park, J.F. Van Guyse, A. Podevyn, E.C. Bolle, N. Bock, E. Linde, M. Celina, R. Hoogenboom, T.R. Dargaville, Influence of side-chain length on long-term release kinetics from poly (2-oxazoline)-drug conjugate networks, Eur. Polym. J. 120 (2019) 109217.
[165] H.S. Yoo, J.E. Oh, K.H. Lee, T.G. Park, Biodegradable nanoparticles containing doxorubicin-PLGA conjugate for sustained release, Pharm. Res. 16 (1999) 1114–1118.
[166] M.F. Seifu, L.K. Nath, Polymer-drug conjugates: novel carriers for cancer chemotherapy, Polym.-Plastics Technol. Mater. 58 (2019) 158–171.
[167] S. Dutta, D.D. Gupta, Conjugation of ibuprofen to poly ethylene glycol and in-vitro drug release evaluation, J. Drug Deliv. Therap. 9 (2019) 110–115.
[168] V. Pawar, M. Dhanka, R. Srivastava, Cefuroxime conjugated chitosan hydrogel for treatment of wound infections, Colloids Surf. B: Biointerfaces 173 (2019) 776–787.
[169] S. Samanta, C.C. De Silva, P. Leophairatana, J.T. Koberstein, Main-chain polyacetal conjugates with HIF-1 inhibitors: temperature-responsive, pH-degradable drug delivery vehicles, J. Mater. Chem. B 6 (2018) 666–674.
[170] R. Cholas, S.K. Padmanabhan, F. Gervaso, G. Udayan, G. Monaco, A. Sannino,

A. Licciulli, Scaffolds for bone regeneration made of hydroxyapatite microspheres in a collagen matrix, Mater. Sci. Eng., C 63 (2016) 499–505.
[171] A.E. Kowalski, T.R. Huber, T.W. Ni, L.F. Hartje, K.L. Appel, J.W. Yost, C.J. Ackerson, C.D. Snow, Gold nanoparticle capture within protein crystal scaffolds, Nanoscale 8 (2016) 12693–12696.
[172] N.A. Peppas, J.J. Sahlin, A simple equation for the description of solute release. III. Coupling of diffusion and relaxation, Int. J. Pharm. 57 (1989) 169–172.
[173] T. Higuchi, Rate of release of medicaments from ointment bases containing drugs in suspension, J. Pharm. Sci. 50 (1961) 874–875.
[174] A. Hixson, J. Crowell, Dependence of reaction velocity upon surface and agitation, Indust. Eng. Chem. 23 (1931) 923–931.
[175] P.L. Ritger, N.A. Peppas, A simple equation for description of solute release II. Fickian and anomalous release from swellable devices, J. Control. Release 5 (1987) 37–42.
[176] P.L. Ritger, N.A. Peppas, A simple equation for description of solute release I. Fickian and non-fickian release from non-swellable devices in the form of slabs, spheres, cylinders or discs, J. Control. Release 5 (1987) 23–36.
[177] S. Zupancic, S. Sinha-Ray, S. Sinha-Ray, J. Kristl, A.L. Yarin, Long-term sustained ciprofloxacin release from pmma and hydrophilic polymer blended nanofibers, Mol. Pharm. 13 (2015) 295–305.
[178] C.G. Pitt, A.R. Jeffcoat, R.A. Zweidinger, A. Schindler, Sustained drug delivery systems. I. The permeability of poly (ε-caprolactone), poly (DL-lactic acid), and their copolymers, J. Biomed. Mater. Res. 13 (3) (1979) 497–507.
[179] Y. Zhou, J. Li, Y. Zhang, D. Dong, E. Zhang, F. Ji, Z. Qin, J. Yang, F. Yao, Establishment of a physical model for solute diffusion in hydrogel: understanding the diffusion of proteins in poly (sulfobetaine methacrylate) hydrogel, J. Phys. Chem. B 121 (2017) 800–814.
[180] B. Amsden, Solute diffusion in hydrogels: an examination of the retardation effect, Polym. Gels Networks 6 (1998) 13–43.
[181] J.P. Schneidér, M.C. Branco, D.J. Pochan, N.J. Wagner, Macromolecular diffusion and release from self-assembled β-hairpin peptide hydrogels, Google Patents, 2014.
[182] Z. Wang, Y. Ren, Y. Zhu, L. Hao, Y. Chen, G. An, H. Wu, X. Shi, C. Mao, A rapidly self-healing host-guest supramolecular hydrogel with high mechanical strength and excellent biocompatibility, Angew. Chem. 130 (2018) 9146–9150.
[183] S.C. Skaalure, U. Akalp, F.J. Vernerey, S.J. Bryant, Tuning reaction and diffusion mediated degradation of enzyme-sensitive hydrogels, Adv. Healthcare Mater. 5 (2016) 432–438.
[184] J. Long, A.V. Nand, S. Ray, S. Mayhew, D. White, C.R. Bunt, A. Seyfoddin, Development of customised 3D printed biodegradable projectile for administrating extended-release contraceptive to wildlife, Int. J. Pharm. 548 (2018) 349–356.
[185] M.C. Branco, D.J. Pochan, N.J. Wagner, J.P. Schneider, Macromolecular diffusion and release from self-assembled β-hairpin peptide hydrogels, Biomaterials 30 (2009) 1339–1347.
[186] J.E. Mealy, C.B. Rodell, J.A. Burdick, Sustained small molecule delivery from injectable hyaluronic acid hydrogels through host–guest mediated retention, J. Mater. Chem. B 3 (2015) 8010–8019.
[187] N. Al-Dubaili, K. El-Tarabily, N.I. Saleh, Host-guest complexes of imazalil with cucurbit [8] uril and β-cyclodextrin and their effect on plant pathogenic fungi, Sci. Reports 8 (2018) 2839.
[188] D.B. Kolesky, R.L. Truby, A.S. Gladman, T.A. Busbee, K.A. Homan, J.A. Lewis, 3D bioprinting of vascularized, heterogeneous cell-laden tissue constructs, Adv. Mater. 26 (2014) 3124–3130.
[189] A. Duarte, A. Martinho, Â. Luís, A. Figueiras, M. Oleastro, F.C. Domingues, F. Silva, Resveratrol encapsulation with methyl-β-cyclodextrin for antibacterial and antioxidant delivery applications, LWT-Food Sci. Technol. 63 (2015) 1254–1260.
[190] S. Phunpee, K. Suktham, S. Surassmo, S. Jarussophon, C. Rungnim, A. Soottitantawat, S. Puttipipatkhachorn, U.R. Ruktanonchai, Controllable encapsulation of α-mangostin with quaternized β-cyclodextrin grafted chitosan using high shear mixing, Int. J. Pharm. 538 (2018) 21–29.
[191] A.G. Guimaraes, M.A. Oliveira, R. dos Santos Alves, P. dos Passos Menezes, M.R. Serafini, A.A. de Souza Araújo, D.P. Bezerra, L.J.Q. Júnior, Encapsulation of carvacrol, a monoterpene present in the essential oil of oregano, with β-cyclodextrin, improves the pharmacological response on cancer pain experimental protocols, Chem. Biol. Interact. 227 (2015) 69–76.
[192] A.S. Al-Jaber, A.D. Bani-Yaseen, On the encapsulation of Olsalazine by β-cyclodextrin: a DFT-based computational and spectroscopic investigations, Spectrochim. Acta Part A Mol. Biomol. Spectrosc. 214 (2019) 531–536.
[193] C.L. Gigliotti, R. Minelli, R. Cavalli, S. Occhipinti, G. Barrera, S. Pizzimenti, G. Cappellano, E. Boggio, L. Conti, R. Fantozzi, In vitro and in vivo therapeutic evaluation of camptothecin-encapsulated β-cyclodextrin nanosponges in prostate cancer, J. Biomed. Nanotechnol. 12 (2016) 114–127.
[194] E.M.P. Garrido, A.S. Cerqueira, D. Chavarria, T. Silva, F. Borges, J.M. Garrido, Microencapsulation of caffeic acid phenethyl ester and caffeic acid phenethyl amide by inclusion in hydroxypropyl-β-cyclodextrin, Food Chem. 254 (2018) 260–265.
[195] C. Dhand, M. Venkatesh, V.A. Barathi, S. Harini, S. Bairagi, E.G.T. Leng, N. Muruganandham, K.Z.W. Low, M.H.U.T. Fazil, X.J. Loh, Bio-inspired cross-linking and matrix-drug interactions for advanced wound dressings with long-term antimicrobial activity, Biomaterials 138 (2017) 153–168.
[196] H. Sun, L. Mei, C. Song, X. Cui, P. Wang, The in vivo degradation, absorption and excretion of PCL-based implant, Biomaterials 27 (2006) 1735–1740.
[197] P. Saini, M. Arora, M.R. Kumar, Poly (lactic acid) blends in biomedical applications, Adv. Drug Deliv. Rev. 107 (2016) 47–59.
[198] N. Saadatkish, S. Nouri Khorasani, M. Morshed, A.R. Allafchian, M.H. Beigi, M. Masoudi Rad, R. Esmaeely Neisiany, M.H. Nasr-Esfahani, A ternary nanofibrous scaffold potential for central nerve system tissue engineering, J. Biomed. Mater. Res. Part A 106 (2018) 2394–2401.
[199] C. Kuang, S. Qavi, R. Foudazi, Double-stage phase separation in dynamically asymmetric ternary polymer blends, RSC Adv. 6 (2016) 92104–92114.
[200] D. David, T. Sincock, Estimation of miscibility of polymer blends using the solubility parameter concept, Polymer 33 (1992) 4505–4514.
[201] J. Gao, S. Chen, D. Tang, L. Jiang, J. Shi, S. Wang, Mechanical properties and degradability of electrospun PCL/PLGA blended scaffolds as vascular grafts, Trans. Tianjin Univ. 25 (2019) 152–160.
[202] H. Van Ngo, P.K. Nguyen, T. Van Vo, W. Duan, V.-T. Tran, P.H.-L. Tran, T.T.-D. Tran, Hydrophilic-hydrophobic polymer blend for modulation of crystalline changes and molecular interactions in solid dispersion, Int. J. Pharm. 513 (2016) 148–152.
[203] B.P. Chang, A.K. Mohanty, M. Misra, Tuning the compatibility to achieve toughened biobased poly (lactic acid)/poly (butylene terephthalate) blends, RSC Adv. 8 (2018) 27709–27724.
[204] M. Alhijjaj, P. Belton, S. Qi, An investigation into the use of polymer blends to improve the printability of and regulate drug release from pharmaceutical solid dispersions prepared via fused deposition modeling (FDM) 3D printing, Eur. J. Pharm. Biopharm. 108 (2016) 111–125.
[205] P. Davoodi, L.Y. Lee, Q. Xu, V. Sunil, Y. Sun, S. Soh, C.-H. Wang, Drug delivery systems for programmed and on-demand release, Adv. Drug Deliv. Rev. (2018).
[206] I. Anna, N. Katarina, Pulsatile release from a flat self-oscillating chitosan macrogel, J. Mater. Chem. B 6 (2018) 5003–5010.
[207] R. Dallmann, S.A. Brown, F. Gachon, Chronopharmacology: new insights and therapeutic implications, Annu. Rev. Pharmacol. Toxicol. 54 (2014) 339–361.
[208] B. Halliwell, Free radicals and other reactive species in disease, Els (2001) 1–9.
[209] C. Wang, J. Wang, X. Zhang, S. Yu, D. Wen, Q. Hu, Y. Ye, H. Bomba, X. Hu, Z. Liu, In situ formed reactive oxygen species–responsive scaffold with gemcitabine and checkpoint inhibitor for combination therapy, Sci. Translat. Med. 10 (2018) eaan3682.
[210] M.K. Gupta, J.R. Martin, T.A. Werfel, T. Shen, J.M. Page, C.L. Duvall, Cell protective, ABC triblock polymer-based thermoresponsive hydrogels with ROS-triggered degradation and drug release, J. Am. Chem. Soc. 136 (2014) 14896–14902.
[211] G.K. Balendiran, R. Dabur, D. Fraser, The role of glutathione in cancer, Cell Biochemistry and Function: Cellular biochemistry and its modulation by active agents or disease 22 (2004) 343–352.
[212] E.H. Cheteh, M. Augsten, H. Rundqvist, J. Bianchi, V. Sarne, L. Egevad, V.J. Bykov, A. Östman, K.G. Wiman, Human cancer-associated fibroblasts enhance glutathione levels and antagonize drug-induced prostate cancer cell death, Cell Death & Disease 8 (2017) e2848.
[213] J. Gan, X. Guan, J. Zheng, H. Guo, K. Wu, L. Liang, M. Lu, Biodegradable, thermoresponsive PNIPAM-based hydrogel scaffolds for the sustained release of levofloxacin, RSC Adv. 6 (2016) 32967–32978.
[214] X. Hu, Y. Wang, L. Zhang, M. Xu, W. Dong, J. Zhang, Redox/pH dual stimuli-responsive degradable Salecan-g-SS-poly (IA-co-HEMA) hydrogel for release of doxorubicin, Carbohydr. Polym. 155 (2017) 242–251.
[215] B.S. McAvan, M. Khuphe, P.D. Thornton, Polymer hydrogels for glutathione-mediated protein release, Eur. Polym. J. 87 (2017) 468–477.
[216] K. Moriyama, K. Minamihata, R. Wakabayashi, M. Goto, N. Kamiya, Enzymatic preparation of a redox-responsive hydrogel for encapsulating and releasing living cells, Chem. Commun. 50 (2014) 5895–5898.
[217] A.L. Lakes, C.T. Jordan, P. Gupta, D.A. Puleo, J.Z. Hilt, T.D. Dziubla, Reducible disulfide poly (beta-amino ester) hydrogels for antioxidant delivery, Acta Biomater. 68 (2018) 178–189.
[218] T. Barroso, R. Viveiros, T. Casimiro, A. Aguiar-Ricardo, Development of dual-responsive chitosan–collagen scaffolds for pulsatile release of bioactive molecules, J. Supercritical Fluids 94 (2014) 102–112.
[219] D. Schmaljohann, J. Oswald, B. Jørgensen, M. Nitschke, D. Beyerlein, C. Werner, Thermo-responsive PNiPAAm-g-PEG films for controlled cell detachment, Biomacromolecules 4 (2003) 1733–1739.
[220] W. Li, J. Wang, J. Ren, X. Qu, 3D graphene oxide–polymer hydrogel: near-infrared light-triggered active scaffold for reversible cell capture and on-demand release, Adv. Mater. 25 (2013) 6737–6743.
[221] M. Zhernenkov, R. Ashkar, H. Feng, O.O. Akintewe, N.D. Gallant, R. Toomey, J.F. Ankner, R. Pynn, Thermoresponsive PNIPAM coatings on nanostructured gratings for cell alignment and release, ACS Appl. Mater. Interfaces 7 (2015) 11857–11862.
[222] A. Adibfar, G. Amoabediny, M.B. Eslaminejad, J. Mohamadi, F. Bagheri, B.Z. Doulabi, VEGF delivery by smart polymeric PNIPAM nanoparticles affects both osteogenic and angiogenic capacities of human bone marrow stem cells, Mater. Sci. Eng., C 93 (2018) 790–799.
[223] B. Dash, Z. Xu, L. Lin, A. Koo, S. Ndon, F. Berthiaume, A. Dardik, H. Hsia, Stem cells and engineered scaffolds for regenerative wound healing, Bioengineering 5 (2018) 23.
[224] A.A. Thorpe, C. Freeman, P. Farthing, J. Callaghan, P.V. Hatton, I.M. Brook, C. Sammon, C.L. Le Maitre, In vivo safety and efficacy testing of a thermally triggered injectable hydrogel scaffold for bone regeneration and augmentation in a rat model, Oncotarget 9 (2018) 18277.
[225] P. Roach, D. McGarvey, M. Lees, C. Hoskins, Remotely triggered scaffolds for controlled release of pharmaceuticals, Int. J. Mol. Sci. 14 (2013) 8585–8602.
[226] A. Alenezi, M. Hulander, S. Atefyekta, M. Andersson, Development of a photon induced drug-delivery implant coating, Mater. Sci. Eng., C 98 (2019) 619–627.
[227] A. Seyfoddin, A. Chan, W.-T. Chen, I. Rupenthal, G. Waterhouse, D. Svirskis, Electro-responsive macroporous polypyrrole scaffolds for triggered

dexamethasone delivery, Eur. J. Pharm. Biopharm. 94 (2015) 419–426.
[228] S.R. Sirsi, M.A. Borden, State-of-the-art materials for ultrasound-triggered drug delivery, Adv. Drug Deliv. Rev. 72 (2014) 3–14.
[229] I. Lentacker, I. De Cock, R. Deckers, S. De Smedt, C. Moonen, Understanding ultrasound induced sonoporation: definitions and underlying mechanisms, Adv. Drug Deliv. Rev. 72 (2014) 49–64.
[230] D.F. Bhutto, E.M. Murphy, M.C. Priddy, C.C. Centner, J.B. Moore IV, R. Bolli, J.A. Kopechek, Effect of Molecular Weight on Sonoporation-Mediated Uptake in Human Cells, Ultrasound Med. Biol. 44 (2018) 2662–2672.
[231] C. Manaspon, C. Hernandez, P. Nittayacharn, S. Jeganathan, N. Nasongkla, A.A. Exner, Increasing distribution of drugs released from in situ forming PLGA implants using therapeutic ultrasound, Ann. Biomed. Eng. 45 (2017) 2879–2887.
[232] C.R. Arciola, Y. An, D. Campoccia, M. Donati, L. Montanaro, Etiology of implant orthopedic infections: a survey on 1027 clinical isolates, Int. J. Artificial Organs 28 (2005) 1091–1100.
[233] C.R. Arciola, D. Campoccia, G.D. Ehrlich, L. Montanaro, Biofilm-based implant infections in orthopaedics, Biofilm-based healthcare-associated infections, Springer, 2015, pp. 29–46.
[234] L. Montanaro, P. Speziale, D. Campoccia, S. Ravaioli, I. Cangini, G. Pietrocola, S. Giannini, C.R. Arciola, Scenery of Staphylococcus implant infections in orthopedics, Future Microbiol. 6 (2011) 1329–1349.
[235] C.R. Arciola, D. Campoccia, L. Montanaro, Implant infections: adhesion, biofilm formation and immune evasion, Nat. Rev. Microbiol. 1 (2018).
[236] M.T. Albuquerque, M.C. Valera, C.S. Moreira, E. Bresciani, R.M. De Melo, M.C. Bottino, Effects of ciprofloxacin-containing scaffolds on enterococcus faecalis biofilms, J. Endodont. 41 (2015) 710–714.
[237] A. Baranowska-Korczyc, A. Warowicka, M. Jasiurkowska-Delaporte, B. Grześkowiak, M. Jarek, B.M. Maciejewska, J. Jurga-Stopa, S. Jurga, Antimicrobial electrospun poly (ε-caprolactone) scaffolds for gingival fibroblast growth, RSC Adv. 6 (2016) 19647–19656.
[238] D. Aydin, M. Arslan, A. Sanyal, R. Sanyal, Hooked on cryogels: a carbamate linker based depot for slow drug release, Bioconjug. Chem. 28 (2017) 1443–1451.
[239] C.J. Bloomquist, M.B. Mecham, M.D. Paradzinsky, R. Januszewicz, S.B. Warner, J.C. Luft, S.J. Mecham, A.Z. Wang, J.M. DeSimone, Controlling release from 3D printed medical devices using CLIP and drug-loaded liquid resins, J. Control. Release 278 (2018) 9–23.
[240] S.H. Lim, S.M.Y. Chia, L. Kang, K.Y.-L. Yap, Three-dimensional printing of carbamazepine sustained-release scaffold, J. Pharm. Sci. 105 (2016) 2155–2163.
[241] A. Mira, C.R. Mateo, R. Mallavia, A. Falco, Poly (methyl vinyl ether-alt-maleic acid) and ethyl monoester as building polymers for drug-loadable electrospun nanofibers, Sci. Rep. 7 (2017) 17205.
[242] M. Mofidfar, J. Wang, L. Long, C.L. Hager, C. Vareechon, E. Pearlman, E. Baer, M. Ghannoum, G.E. Wnek, Polymeric nanofiber/antifungal formulations using a novel co-extrusion approach, AAPS PharmSciTech 18 (2017) 1917–1924.
[243] K.P. Murphy, M.A. Hendley, C. Isely, P. Annamalai, E. Peña, R.M. Gower, Resveratrol delivery from porous poly (lactide-co-glycolide) scaffolds promotes an anti-inflammatory environment within visceral adipose tissue, ACS Appl. Mater. Interfaces 10 (2018) 43363–43374.
[244] R. Shi, Y. Huang, J. Zhang, C. Wu, M. Gong, W. Tian, L. Zhang, Effective delivery of mitomycin-C and meloxicam by double-layer electrospun membranes for the prevention of epidural adhesions, J. Biomed. Mater. Res. Part B: Appl. Biomater. (2019).
[245] L.E. Visscher, H.P. Dang, M.A. Knackstedt, D.W. Hutmacher, P.A. Tran, 3D printed Polycaprolactone scaffolds with dual macro-microporosity for applications in local delivery of antibiotics, Mater. Sci. Eng., C 87 (2018) 78–89.
[246] J. Xue, Y. Niu, M. Gong, R. Shi, D. Chen, L. Zhang, Y. Lvov, Electrospun microfiber membranes embedded with drug-loaded clay nanotubes for sustained antimicrobial protection, ACS Nano 9 (2015) 1600–1612.
[247] S. Baron, Classification–Medical Microbiology, University of Texas Medical Branch at Galveston, 1996.
[248] D. Byarugaba, Antimicrobial resistance in developing countries and responsible risk factors, Int. J. Antimicrob. Agents 24 (2004) 105–110.
[249] P.W. Taylor, P.D. Stapleton, J.P. Luzio, New ways to treat bacterial infections, Drug Discov. Today 7 (2002) 1086–1091.
[250] B.S. Okan, A. Marset, J. Seyyed Monfared Zanjani, P.A. Sut, O. Sen, M. Çulha, Y. Menceloglu, Thermally exfoliated graphene oxide reinforced fluorinated pentablock poly (l-lactide-co-ε-caprolactone) electrospun scaffolds: Insight into antimicrobial activity and biodegradation, J. Appl. Polym. Sci. 133 (2016).
[251] Y. Ding, W. Li, A. Correia, Y. Yang, K. Zheng, D. Liu, D.W. Schubert, A.R. Boccaccini, H.l.A. Santos, J.A. Roether, Electrospun polyhydroxybutyrate/poly (ε-caprolactone)/sol–gel-derived silica hybrid scaffolds with drug releasing function for bone tissue engineering applications, ACS Appl. Mater. Interfaces 10 (2018) 14540–14548.
[252] M.G. Tardajos, G. Cama, M. Dash, L. Misseeuw, T. Gheysens, C. Gorzelanny, T. Coenye, P. Dubruel, Chitosan functionalized poly-ε-caprolactone electrospun fibers and 3D printed scaffolds as antibacterial materials for tissue engineering applications, Carbohydr. Polym. 191 (2018) 127–135.
[253] M.O. Freire, T.E. Van Dyke, Natural resolution of inflammation, Periodontology 2000 (63) (2013) 149–164.
[254] B. Jonsson, B. Stromqvist, Repeat decompression of lumbar nerve roots. A prospective two-year evaluation, J. Bone Joint Surgery. British 75 (1993) 894–897.
[255] J.-Y. Lee, W. Stenzel, H. Ebel, C. Wedekind, R.-I. Ernestus, N. Klug, Mitomycin C in preventing spinal epidural fibrosis in a laminectomy model in rats, J. Neurosurgery: Spine 100 (2004) 52–55.
[256] M. Griffith, M.M. Islam, J. Edin, G. Papapavlou, O. Buznyk, H.K. Patra, The quest for anti-inflammatory and anti-infective biomaterials in clinical translation, Front. Bioeng. Biotechnol. 4 (2016) 71.
[257] J.C. Fernandes, H. Spindola, V. De Sousa, A. Santos-Silva, M.E. Pintado, F.X. Malcata, J.E. Carvalho, Anti-inflammatory activity of chitooligosaccharides in vivo, Mar. Drugs 8 (2010) 1763–1768.
[258] M. Yousef, R. Pichyangkura, S. Soodvilai, V. Chatsudthipong, C. Muanprasat, Chitosan oligosaccharide as potential therapy of inflammatory bowel disease: therapeutic efficacy and possible mechanisms of action, Pharmacol. Res. 66 (2012) 66–79.
[259] S. Kim, J.E. Jang, J.H. Lee, G. Khang, Composite scaffold of micronized porcine cartilage/poly (lactic-co-glycolic acid) enhances anti-inflammatory effect, Mater. Sci. Eng., C 88 (2018) 46–52.
[260] A.L. Zachman, S.W. Crowder, O. Ortiz, K.J. Zienkiewicz, C.M. Bronikowski, S.S. Yu, T.D. Giorgio, S.A. Guelcher, J. Kohn, H.-J. Sung, Pro-angiogenic and anti-inflammatory regulation by functional peptides loaded in polymeric implants for soft tissue regeneration, Tissue Eng. Part A 19 (2012) 437–447.
[261] D. Wu, X. Chen, T. Chen, C. Ding, W. Wu, J. Li, Substrate-anchored and degradation-sensitive anti-inflammatory coatings for implant materials, Sci. Rep. 5 (2015) 11105.
[262] T.J. Cho, L.C. Gerstenfeld, T.A. Einhorn, Differential temporal expression of members of the transforming growth factor β superfamily during murine fracture healing, J. Bone Miner. Res. 17 (2002) 513–520.
[263] B.-B. Seo, J.-T. Koh, S.-C. Song, Tuning physical properties and BMP-2 release rates of injectable hydrogel systems for an optimal bone regeneration effect, Biomaterials 122 (2017) 91–104.
[264] S.-F. Chou, K.A. Woodrow, Relationships between mechanical properties and drug release from electrospun fibers of PCL and PLGA blends, J. Mech. Behav. Biomed. Mater. 65 (2017) 724–733.
[265] P. Tayalia, D.J. Mooney, Controlled growth factor delivery for tissue engineering, Adv. Mater. 21 (2009) 3269–3285.
[266] Z. Wang, Z. Wang, W.W. Lu, W. Zhen, D. Yang, S. Peng, Novel biomaterial strategies for controlled growth factor delivery for biomedical applications, NPG Asia Mater. 9 (2017) e435.
[267] S. Mohammadi, S. Ramakrishna, S. Laurent, M.A. Shokrgozar, D. Semnani, D. Sadeghi, S. Bonakdar, M. Akbari, Fabrication of nanofibrous PVA/alginate-sulfate substrates for growth factor delivery, J. Biomed. Mater. Res. Part A 107 (2019) 403–413.
[268] P.V. Mummaneni, J. Pan, R.W. Haid, G.E. Rodts, Contribution of recombinant human bone morphogenetic protein—2 to the rapid creation of interbody fusion when used in transforaminal lumbar interbody fusion: a preliminary report: Invited submission from the Joint Section Meeting on Disorders of the Spine and Peripheral Nerves, March 2004, J. Neurosurgery: Spine 1 (1) (2004) 19–23.
[269] H.J. Meisel, M. Schnöring, C. Hohaus, Y. Minkus, A. Beier, T. Ganey, U. Mansmann, Posterior lumbar interbody fusion using rhBMP-2, Eur. Spine J. 17 (12) (2008) 1735–1744.
[270] S. Hershman, L.G. Jenis, BMP 2 usage in posterior lumbar fusion in degenerative conditions, Seminars in Spine Surgery, Elsevier, 2016, pp. 239–244.
[271] C.K. Griffith, C. Miller, R.C. Sainson, J.W. Calvert, N.L. Jeon, C.C. Hughes, S.C. George, Diffusion limits of an in vitro thick prevascularized tissue, Tissue Eng. 11 (2005) 257–266.
[272] K.S. Cahill, J.H. Chi, A. Day, E.B. Claus, Prevalence, complications, and hospital charges associated with use of bone-morphogenetic proteins in spinal fusion procedures, JAMA 302 (1) (2009) 58–66.
[273] A.T. Villavicencio, S. Burneikiene, RhBMP-2-induced radiculitis in patients undergoing transforaminal lumbar interbody fusion: relationship to dose, Spine J. 16 (10) (2016) 1208–1213.
[274] C.A. Tannoury, H.S. An, Complications with the use of bone morphogenetic protein 2 (BMP-2) in spine surgery, Spine J. 14 (3) (2014) 552–559.
[275] J. Zhang, J. Li, G. Jia, Y. Jiang, Q. Liu, X. Yang, S. Pan, Improving osteogenesis of PLGA/HA porous scaffolds based on dual delivery of BMP-2 and IGF-1 via a polydopamine coating, RSC Adv. 7 (2017) 56732–56742.
[276] F.-M. Chen, R. Chen, X.-J. Wang, H.-H. Sun, Z.-F. Wu, In vitro cellular responses to scaffolds containing two microencapulated growth factors, Biomaterials 30 (2009) 5215–5224.
[277] S. Kim, Y. Kang, C.A. Krueger, M. Sen, J.B. Holcomb, D. Chen, J.C. Wenke, Y. Yang, Sequential delivery of BMP-2 and IGF-1 using a chitosan gel with gelatin microspheres enhances early osteoblastic differentiation, Acta Biomater. 8 (2012) 1768–1777.
[278] J. Siedlecki, C. Wertheimer, A. Wolf, R. Liegl, C. Priglinger, S. Priglinger, K. Eibl-Lindner, Combined VEGF and PDGF inhibition for neovascular AMD: anti-angiogenic properties of axitinib on human endothelial cells and pericytes in vitro, Graefe's Arch. Clin. Exp. Ophthalmol. 255 (2017) 963–972.
[279] G.A. Rico-Llanos, J. Becerra, R. Visser, Insulin-like growth factor-1 (IGF-1) enhances the osteogenic activity of bone morphogenetic protein-6 (BMP-6) in vitro and in vivo, and together have a stronger osteogenic effect than when IGF-1 is combined with BMP-2, J. Biomed. Mater. Res. Part A 105 (2017) 1867–1875.
[280] F. Sharmin, C. McDermott, J. Lieberman, A. Sanjay, Y. Khan, Dual growth factor delivery from biofunctionalized allografts: Sequential VEGF and BMP-2 release to stimulate allograft remodeling, J. Orthop. Res. 35 (2017) 1086–1095.
[281] D.H. Kempen, L. Lu, A. Heijink, T.E. Hefferan, L.B. Creemers, A. Maran, M.J. Yaszemski, W.J. Dhert, Effect of local sequential VEGF and BMP-2 delivery on ectopic and orthotopic bone regeneration, Biomaterials 30 (2009) 2816–2825.
[282] S. Zhang, J. Chen, Y. Yu, K. Dai, J. Wang, C. Liu, Accelerated bone regenerative efficiency by regulating sequential release of BMP-2 and VEGF and synergism with sulfated chitosan, ACS Biomater. Sci. Eng. (2019).